Biogeosciences Discuss., doi:10.5194/bg-2017-160, 2017
Manuscript under review for journal Biogeosciences
Discussion started: 19 May 2017

Biogeosciences Discussions Open Access EGU

Global consequences of afforestation and bioenergy cultivation on ecosystem service indicators

Andreas Krause[1], Anita D. Bayer[1], Thomas A. M. Pugh[1,2], Jonathan C. Doelman[3], Florian Humpenöder[4], Peter Anthoni[1], Stefan Olin[5], Benjamin L. Bodirsky[4], Alexander Popp[4], Elke Stehfest[3], Almut Arneth[1]

[1]Karlsruhe Institute of Technology, Institute of Meteorology and Climate Research – Atmospheric Environmental Research (IMK-IFU), Kreuzeckbahnstr. 19, Garmisch-Partenkirchen, 82467, Germany

[2]School of Geography, Earth & Environmental Science and Birmingham Institute of Forest Research, University of Birmingham, Birmingham, B15 2TT, United Kingdom

[3]PBL, Netherlands Environmental Assessment Agency, 2500 GH The Hague, Postbus 30314, Netherlands

[4]Potsdam Institute for Climate Impact Research (PIK), Telegrafenberg, PO Box 60 12 03, Potsdam, 14412, Germany

[5]Department of Physical Geography and Ecosystem Science, Lund University, Lund, 22362, Sweden

Correspondence to: Andreas Krause (andreas.krause@kit.edu)

Abstract. Land management for carbon storage is discussed as being indispensable for climate change mitigation because of its large potential to remove carbon dioxide from the atmosphere, and to avoid further emissions from deforestation. However, land-based mitigation's prospect of success depends on potential side-effects on important ecosystem services. Here, we use projections of future land use and land cover for different land-based mitigation options from two land-use models (IMAGE and MAgPIE) and evaluate their effects with a global dynamic vegetation model (LPJ-GUESS). In the land-use models, a cumulative carbon removal target of 130 GtC by the end of the 21st century was set to be achieved either via growth of bioenergy crops combined with carbon capture and storage, via avoided deforestation and afforestation, or via a combination of both. We compare these scenarios to a reference scenario without land-based mitigation and analyse the LPJ-GUESS simulations with the aim to assess synergies and trade-offs across a range of ecosystem service indicators: carbon sequestration, surface albedo, evapotranspiration, water runoff, crop production, nitrogen loss, and emissions of biogenic volatile organic compounds.

In our mitigation simulations carbon removal by year 2099 ranged between 55 and 89 GtC, and thus lower than the removal simulated by the land-use models. Other ecosystem service indicators were influenced heterogeneously both positively and negatively, with large variability across regions and land-use scenarios. Avoided deforestation and afforestation led to an increase in evapotranspiration and enhanced emissions of biogenic volatile organic compounds, and to a decrease in albedo, runoff, and nitrogen loss. Also crop production decreased in the afforestation scenario as a result of reduced crop area,

Biogeosciences Discuss., doi:10.5194/bg-2017-160, 2017
Manuscript under review for journal Biogeosciences
Discussion started: 19 May 2017

especially for MAgPIE land-use patterns. Bioenergy-based climate change mitigation was projected to affect less area globally than in the forest expansion scenarios, and resulted in less pronounced changes in most ecosystem service indicators than forest-based mitigation, but included a decrease in crop production, nitrogen loss and biogenic volatile organic compounds emissions.

1 Introduction

If the trend in global carbon dioxide (CO_2) emissions observed over the last two decades continues, the atmospheric CO_2 concentration is expected to exceed 900 ppm at the end of the 21st century resulting in a surface temperature increase of several degrees (Friedlingstein et al., 2014;Le Quere et al., 2015;Peters et al., 2013). However, during the COP21 climate conference in Paris 2015, participating parties agreed to limit global warming to 2° C or less relative to the preindustrial era, and by today, 144 countries have ratified the agreement (http://unfccc.int/paris_agreement/items/9485.php, accessed 26 April 2017). The <2°C warming goal requires greenhouse gas (GHG) concentrations to approximately follow or stay below the representative concentration pathway 2.6 (RCP2.6, van Vuuren et al., 2011), which will require serious reductions in CO_2 (and other GHG) emissions across all sectors. Present projections indicate that without substantial net negative CO_2 emissions later during this century the Paris goal will not be achievable (Fuss et al., 2014;Rogelj et al., 2015), and that some negative emissions need to be realized in 10-20 years already (Anderson and Peters, 2016).

The total carbon dioxide removal (CDR) necessary to achieve the 2° C target has been estimated to be at least 25-100 GtC by the end of this century but could be as high as 800 GtC (Gasser et al., 2015), depending on the actual future CO_2 emission pathway and including the need to avoid carbon (C) emissions from further land clearance. Two main strategies of land-based climate change mitigation are commonly discussed for CDR: growth of bioenergy crops in combination with carbon capture and storage (BECCS), and avoided deforestation in combination with afforestation and reforestation (ADAFF) (Humpenöder et al., 2014;van Vuuren et al., 2013;Williamson, 2016). BECCS involves the planting of bioenergy crops or trees, which are burned in power stations or converted to biofuels, and the released CO_2 being captured for long-term underground storage in geological reservoirs. ADAFF utilizes the natural C uptake of forest ecosystems in biomass and soil by maintaining and expanding global forest area.

The total land demand for these mitigation strategies is highly uncertain due to strong dependencies on underlying assumptions about future environmental and socio-economic changes (Popp et al., 2017;Slade et al., 2014). BECCS and ADAFF will likely increase pressure on food-producing agricultural areas and, in the case of BECCS, natural ecosystems. Moreover, similar to other mitigation technologies, the practicability and effectivity of BECCS and ADAFF are debated (Keller et al., 2014;Williamson, 2016). For instance, in boreal and many temperate regions tree cover reduces surface albedo, thereby causing local warming (Alkama and Cescatti, 2016). Additionally, reduced CO_2 emissions through forest protection

might be counteracted by cropland expansion in non-forest areas (Popp *et al.*, 2014). BECCS will create substantial economic costs in its CCS component (Smith et al., 2016) and is far from being deployable at the commercial scale (Peters et al., 2017;Reiner, 2016). It will also require sufficient safe geologic C storage capacities (Scott et al., 2015). Additionally, the efficiency of BECCS might diminish when C emissions from deforestation (Wiltshire and Davies-Barnard, 2015) or nitrous oxide (N_2O) emissions from bioenergy crops (Crutzen et al., 2008) are considered.

But even if land-based measures were to be successful with respect to their primary goal of permanently and substantially reducing atmospheric CO_2 levels to mitigate climate change, impacts on ecosystems and societies are likely to be complex (Bennett et al., 2009;Creutzig et al., 2015;Foley et al., 2005;Smith and Torn, 2013;Smith et al., 2013;Viglizzo et al., 2012) and include effects far away from the original land-use (LU) location (DeFries et al., 2004;Rodriguez et al., 2006). The multiplicity of environmental implications caused by large-scale CO_2 removal have so far been largely neglected (Williamson, 2016). The relevance of negative emission technologies, combined with our limited knowledge of their feasibility and risks, encourages the exploration of potential synergies and trade-offs between terrestrial ecosystem services (ES, defined as benefits that people obtain from ecosystems, MEA, 2005) that are affected in land-based mitigation projects. Such work will facilitate decision-making as to whether the realization of such projects is desirable for society.

In this study, we utilize projections of future LU from one Integrated Assessment Model (IAM, IMAGE) and one LU model (MAgPIE), that are created based on three large-scale land-based mitigation scenarios. Each of these target a CDR of 130 GtC by the end of the century, which is approximately equivalent to the cumulative deforestation CO_2 emissions from the late 19th century to today, or around 60 ppm (Le Quere et al., 2015). We use these spatially explicit LU patterns as input for simulations with the LPJ-GUESS dynamic vegetation model to analyse effects on a variety of ecosystem functions that serve as indicators for important ecosystem services. This is to our knowledge the first time that global LU scenarios from LU models (which are coupled to a vegetation model, in both cases LPJmL) are being used as input to a process-based ecosystem model to assess changes in ecosystem function and effects on multiple ES indicators.

2 Methods

2.1 LPJ-GUESS

The processed-based dynamic global vegetation model (DGVM) LPJ-GUESS simulates vegetation dynamics in response to climate, LU, atmospheric CO_2 and nitrogen (N) input (Olin et al., 2015a;Smith et al., 2014). The model distinguishes between natural, pasture and cropland land-cover types (Lindeskog et al., 2013), all of which include C-N dynamics (Olin et al., 2015a;Smith et al., 2014). Vegetation dynamics in natural land cover are characterized by the establishment, competition

and mortality of twelve plant functional types (PFTs, ten groups of tree species, C3 and C4 grasses) in a number of replicate patches (10 in this study for primary vegetation, 2 for abandoned agricultural areas). Pastures are populated by C3 or C4 grasses which are annually harvested (50% of above-ground biomass) (Lindeskog et al., 2013). Croplands are represented by prescribed fractions of five crop functional types (CFTs, see Table A1) which are fertilized, irrigated, tilled and harvested (Olin et al., 2015a). While LPJ-GUESS does not assume yield increases due to technological progress (in contrast to the LUMs), climate change adaption is simulated by using a dynamic potential heat unit (PHU) calculation (Lindeskog et al., 2013). The PHU sum needed for the full development of a crop determines its harvesting time. For irrigated crops, water supply is assumed to be available as required to fulfil the plant's water demand. Unmanaged cover grass (C3 or C4 type depending on climate) is allowed to grow in croplands between growing seasons.

2.2 The IMAGE and MAgPIE models and the provided land-use scenarios

IMAGE is an IAM model frameworks that includes several sub-models representing the energy system, agricultural economy, LU, natural vegetation and the climate system (Stehfest et al., 2014). Socio-economic parameters are usually calculated for 26 world regions, and most environmental parameters are modelled on a 0.5° x 0.5° grid at annual time steps. LU dynamics are driven by demand for and supply of crops, animal products and bioenergy. Bioenergy demand to achieve a specific CDR target is determined by the energy system sub-model which uses land availability from the LU sub-model following a set of sustainability criteria (Hoogwijk et al., 2003). For this study, bioenergy crops are included as fast growing C4 grasses (Doelman et al., submitted) as these produce higher yields than woody plants in many locations. The level of agricultural intensification required to free up land for afforestation to achieve a specific CDR target is estimated using a stepwise approach of increasing yields and livestock efficiencies. This implies that reduced crop and pasture areas go with higher yields and livestock efficiencies, thereby allowing the same food production as in the baseline. Afforestation is assumed to occur first in grid-cells with high potential for forest growth. IMAGE also represents degraded areas (calibrated so that, together with areas cleared for agriculture, FAO deforestation statistics are met) which can be reforested as part of the afforestation activities (Doelman et al., submitted). Natural vegetation regrowth trajectories and also crop yields, C and water dynamics are modelled dynamically by the DGVM LPJmL (Bondeau et al., 2007;Stehfest et al., 2014).

MAgPIE is a global multi-regional partial equilibrium model of the agricultural sector (Lotze-Campen et al., 2008;Popp et al., 2014). The model aims to minimize the global costs for agricultural production throughout the 21st century at a 5-year time step (recursive dynamic optimization) and is driven by demand for agricultural commodities and associated costs in ten world regions. The cost minimization is subject to various spatially explicit biophysical factors such as land and water availability as well as crop yields (provided by LPJmL). Major options to fulfil increasing demand are intensification (yield-increasing technologies), expansion (LU change) and international trade. Demand for CDR enters the model at the global scale, while the spatial distribution of bioenergy production or afforestation is derived endogenously in the model (involving

economic and biophysical factors). Bioenergy demand is fulfilled chiefly through the growth and harvest of grassy energy crops; woody bioenergy in this study is grown only on less than 1% of the area used for bioenergy. Actual bioenergy yields are derived from potential LPJmL yields (using information about observed LU intensity and agricultural area for initialization) but can exceed LPJmL yields over time due to technological progress (Humpenöder et al., 2014). Afforestation is assumed to occur as managed re-growth of natural vegetation according to parameterized s-shaped growth curves towards a maximum potential natural vegetation C density as provided by LPJmL, with soil C increasing linearly towards its potential maximum within 20 years (Humpenöder et al., 2014). For simplicity, we refer to both IMAGE and MAgPIE as LU models (LUMs) in the following.

As input to our study we used the baseline projections from IMAGE and MAgPIE, and three land-based mitigation scenarios, each calculated by both LUMs, which were all based on the assumption of a cumulative CDR target of 130 GtC by the year 2100. In the "BECCS" scenario this was achieved via bioenergy plant cultivation and subsequent CCS, the "ADAFF" scenario involved maintaining and expanding of global forest area and in "BECCS-ADAFF" the CDR demand was fulfilled in equal parts via both options. While the CDR target in ADAFF was achieved via terrestrial C uptake (CDR = Δ vegetation C + Δ soil C), in BECCS it was fulfilled solely via CSS (CDR = cumulative CCS) and thus did not account for changes in vegetation and soil C. The baseline scenario ("BASE") involved no land-based mitigation but land-use change (LUC) took place in response to, e.g. increasing food demand, GDP growth, and technological changes. All of these scenarios were developed with RCP2.6 climate produced by the IPSL-CM5A-LR general circulation model (GCM), bias corrected to the 1960-1999 historical period (Hempel et al., 2013). As it seems currently unlikely that the RCP2.6 pathway can be achieved without any land-based mitigation, the BASE scenario should rather be regarded as a diagnostic scenario to isolate the LU effects induced by the mitigation scenarios from other factors. CO_2 fertilization effects on plant growth were simulated in the LUMs' crop growth and vegetation models. Both LUMs harmonized their cropland and pasture LU patterns to the spatially explicit HYDE 3.1 dataset (Klein Goldewijk et al., 2011) in the year 1995 (MAgPIE) or 2005 (IMAGE), with small differences in the area of different land cover classes occurring due to different land masks and calibration routines. Socio-economic developments as input to the LUMs were based on the Shared Socio-economic Pathway 2 (SSP2, "Middle of the Road") (O'Neill et al., 2014, Popp et al., 2017). We only used spatially explicit LU and land management (irrigation and synthetic and organic N fertilizer) patterns from the LUMs as input to the LPJ-GUESS simulations, other variables also available from the LUMs (e.g. C stocks or crop production) were calculated with LPJ-GUESS. Details about the conversion of IMAGE and MAgPIE LU data to LPJ-GUESS input data can be found in the Appendix A.

Even though MAgPIE and IMAGE derive crop yields and C densities from the same DGVM (LPJmL; Bondeau et al., 2007), the land demand to meet the same CDR target is larger in IMAGE than in MAgPIE. This reflects different model approaches: While in IMAGE bioenergy cultivation can only be established in unproductive regions not needed for food production, in MAgPIE there is a competition for land between food production and land-based mitigation. Concerning

afforestation, managed regrowth is assumed in MAgPIE while in IMAGE natural succession dynamically calculated within LPJmL is implemented. Consequently, bioenergy production in MAgPIE is located in regions with higher yields compared to IMAGE, and forest regrowth occurs at a faster rate, resulting in less LUC in all MAgPIE scenarios (Fig. 1, Table A2). In the BASE scenario, the area under natural vegetation decreases throughout the future for both IMAGE and MAgPIE (Fig. 1, Table A2), but more so for IMAGE due to the representation of degraded forests (which are treated as pastures, see appendix A). Substantial regional differences between both LUMs exist by the end of the century in the BASE scenario (Fig. 2a). Avoided deforestation and afforestation in the ADAFF scenarios is concentrated in the tropics (Fig. 2b). The area under natural vegetation decreases for the BECCS scenarios, including substantial regional differences (Fig. 2c), but increases for BECCS-ADAFF (Fig. 1). IMAGE uses a slightly larger grid-list than MAgPIE and accounts for the water fraction of a grid-cell; but as the impacts on land-based mitigation in LPJ-GUESS turned out to be small (<2 GtC over the simulation period) we only included grid-cells in our simulations for which LU data was provided by both LUMs (assuming 100% land cover) to facilitate comparison of the results.

2.3 The IMAGE and MAgPIE models and the provided land-use scenarios

The LPJ-GUESS simulations were forced by daily atmospheric climate variables (surface temperature, precipitation, short-wave radiation) extracted from bias-corrected simulated IPSL-CM5A-LR RCP2.6 climate (1950-2099) from the first phase of ISI-MIP project (Warszawski et al., 2014). For the historical period we randomly chose years from the period 1950-1959 to generate climate data for the years 1901-1949. A repeating climate cycle from the 1901-1930 period was used for the model's spin-up. The global average surface temperature increase in IPSL-CM5A-LR is 1.3°C (1.6°C on land) by the end of the century (2070-2099) compared to present-day (1980-2009) for RCP2.6. This value is in the middle of an ensemble of a wider range of GCM models used in ISI-MIP (Warszawski et al., 2014). Historical (1901-2005) and future (RCP2.6, 2005-2099) atmospheric CO_2 mixing ratios were taken from Meinshausen et al. (2011). The year 1901 value (296 ppmv) was used for the spin-up. Future atmospheric CO_2 mixing ratio peaks at 443 ppmv in year 2052 and drops to ~424 ppmv by the end of the century (Meinshausen et al., 2011). Gridded N deposition rates were available as decadal monthly averages for the historical and future (RCP2.6) period (Lamarque et al., 2010;Lamarque et al., 2011). N deposition for year 1901 was used for the spin-up. Spatially explicit LU patterns and N fertilization were adopted from IMAGE and MAgPIE (see also Appendix A). We used the year 1901 land cover map for the spin-up, thereby omitting LUC occurring before the 20th century as we assumed legacy effects from pre-1900 LUC on the future C cycle to be small.

2.4 Analysed ecosystem service indicators

We analysed the implications of future LU patterns for the following ES indicators: C storage (as an indicator for global climate change mitigation), surface albedo and evapotranspiration (indicators for regional climate effects in response to land cover change), annual runoff (indicator for water availability), peak monthly runoff (indicator for flood protection), crop

production (excluding cotton, forage crops, and pasture harvest; indicator for food production), N loss (in LPJ-GUESS currently not differentiated into dissolved N *vs.* N lost to the atmosphere; indicator for water or air quality, or GHG losses), and emissions of the most common biogenic volatile organic compounds (BVOCs) - isoprene and monoterpenes (indicator for air quality). In some cases, ES indicators could be interpreted as proxies for several ES. Most of these variables are direct outputs from LPJ-GUESS simulations. Calculations for ES indicators not taken directly from model outputs (C storage via CCS, crop production scaled to EarthStat, albedo) or differed from the standard model setup (BVOCs) are provided in the Appendix B-E.

3 Results

In the following, the expressions "IMAGE" and "MAgPIE" refer to results from LPJ-GUESS simulations driven by LU patterns from the IMAGE and MAgPIE LUMs, plus climate, CO_2, and N deposition from RCP2.6. In the discussion section at some points we refer to output directly taken from the IMAGE and MAgPIE scenarios, in which case this is explicitly stated ("directly from the LUMs /the LUMs report").

3.1 Carbon storage

Total global C pools simulated with LPJ-GUESS are generally lower for IMAGE than for MAgPIE LU patterns for all scenarios (Table 1, Fig. A1a). This difference is mainly a result of the representation of degraded forests as grasslands in IMAGE LU patterns (see Table A2), while MAgPIE does not include degraded forests. Moreover, some temperate croplands that are specified in the MAgPIE LU patterns to grow fodder are represented in LPJ-GUESS by rain-fed or irrigated, harvested grass. This crop type increases soil C relative to cereals because the larger below-ground/above-ground ratio results in less C being removed during harvest and thus more C input to the soil. C sequestration is calculated by LPJ-GUESS for both BASE simulations within the 21st century, resulting in total C pools of 1995 (IMAGE) and 2047 (MAgPIE) GtC by 2090-2099 (Table 1). The combined effects of LU, changing climate, N deposition, and atmospheric CO_2 levels thus enhance total C pools by ~1.7% and 3.2% (33 and 64 Gt) between the beginning and the end of the century (Fig. 3a).

As expected from the overall scenario objective, total, vegetation, and soil C pools are higher in the ADAFF simulations than in BASE at the end of the century (Table 1, Fig. A1a-c). The additional C uptake is larger for IMAGE (3.6% or 72 GtC in year 2090-2099, 76 GtC in year 2099) than for MAgPIE (2.4% or 49 GtC in year 2090-2099, 55 GtC in year 2099, Fig. 3b). This reflects the larger afforestation area in IMAGE (Fig. 1, Fig. 2b). The largest changes in total C are found in tropical regions, especially in Africa (+15% and +9%, Fig. 4b), respectively tropical forests (+13% and +8%, Fig. A2b), mostly due to increases in vegetation C. Still, the total C uptake of 76 GtC in IMAGE ADAFF compared with the BASE simulation (55

GtC in the MAgPIE case) is well below the CDR target of 130 GtC that underlies the LU scenarios, which is presumably mainly a result of less soil C uptake in LPJ-GUESS.

The BECCS scenario focusing on bioenergy crops and CCS as a climate change mitigation strategy removes slightly less C from the atmosphere than ADAFF (both compared to BASE 2090-2099) for IMAGE LU patterns but removes more C for MAgPIE (Table 1, Fig. 3c). Interestingly, IMAGE ADAFF accumulates more C than IMAGE BECCS within the first half of the century, while BECCS is then catching up during the second half of the century (Fig. A1a); this acceleration of BECCS sink is related to a steady increase in bio-energy area throughout the century. The additional total C storage achieved by the period 2090-2099 (compared to BASE 2090-2099) is 66 GtC (74 GtC in year 2099) for IMAGE and 61 GtC (69 GtC in year 2099) for MAgPIE. Within these totals, cumulative C storage via CCS is 100 GtC and 74 GtC by the end of the century (Table 1), but total C uptake is less than cumulative CCS as LPJ-GUESS simulates a loss of vegetation and soil C from expanded agricultural land. C storage in the combined bioenergy/avoided deforestation and afforestation case (BECCS-ADAFF) most of the time lies between the BECCS and the ADAFF case but for IMAGE exceeds both ADAFF and BECCS by the end of the century (Table 1, Fig. 3d, Fig. A1a, Fig. A3).

3.2 Albedo

Globally averaged January albedo under present-day conditions is significantly higher (~0.25) than July albedo (~0.18) due to the extensive northern-hemisphere snow cover in January. Both values decrease throughout the 21st century in the BASE simulations, but more so for January (-4.1% and -3.7% for IMAGE, respectively MAgPIE) than for July (-1.7% and -1.8%) as a result of northward vegetation shifts and reductions in snow cover (Table 1, Fig. 3a, Fig. A1d-e). For both months and both LUMs, greatest reductions occur in high latitudes (Fig. 4a).

An increase in forested area as in the ADAFF scenario results in further albedo reductions that are - at least for July albedo - comparable in magnitude to the changes in BASE throughout the century (Table 1, Fig. 3b). Only small increases compared to BASE occur in the BECCS simulations (Fig. 3c) as the land demand for bioenergy crop cultivation is relatively small. BECCS-ADAFF results in a decrease in January and July albedo for both LUMs.

3.3 Evapotranspiration

Global evapotranspiration in the BASE simulations decreases much more for IMAGE (-1.2%) than for MAgPIE (0.1%; Table 1, Fig 3a, Fig. A1f). There is large spatial variability with evapotranspiration decreasing in some regions but increasing in others (Fig. 4a), mainly driven by shifting rainfall patterns (not shown).

Biogeosciences Discuss., doi:10.5194/bg-2017-160, 2017
Manuscript under review for journal Biogeosciences
Discussion started: 19 May 2017

As expected from the generally high evapotranspiration rates of forests, end-of-century evapotranspiration in ADAFF is 2.1% and 1.3% higher than in BASE for IMAGE and MAgPIE, respectively (Fig. 3b), with the largest increase occurring in Africa (Fig. 4b). BECCS results in a change of -0.4% and +0.2% for IMAGE, respectively MAgPIE, and BECCS-ADAFF in an increase of 1.3% and 0.8% compared to BASE.

3.4 Runoff

In the BASE simulations, global annual runoff increases by 4.9% and 4.1% until the end of the century for IMAGE, respectively MAgPIE, with a slightly larger increase of 5.2% and 5.0% in peak monthly runoff (Table 1, Fig. 3a). This increase is mainly driven by precipitation changes, but forest loss and increased water use efficiency simulated under elevated CO_2 levels also play a role. Similar to evapotranspiration, spatial patterns are heterogeneous, with generally larger changes in annual runoff than in peak monthly runoff in high latitudes and reverse patterns in parts of the (sub)tropics (Fig. 4a, Fig. A2a).

Changes in runoff in the mitigation simulations are opposite to evapotranspiration changes (Fig. 3b-d, Fig. 4b-c) and the effects of land-based mitigation on annual runoff are often larger than on peak monthly runoff. ADAFF reduces annual runoff by 2.2% and 1.1% (IMAGE and MAgPIE) and peak monthly runoff by 1.3% and 0.7%, while BECCS increases annual runoff by 0.3% and 0.2% and peak monthly runoff by 0.2% and 0.0%.

3.5 Crop Production

Globally, total crop production simulated by LPJ-GUESS averages ~29 and 27 Ecal yr^{-1} over the years 2000-2009 and increases to 36 and 45 Ecal yr^{-1} by the end of the century for the IMAGE, respectively MAgPIE, BASE simulation (Table 1, Fig. A1i), while it increases by 78% and 96% in the original LUM results. The large differences in crop production increase between IMAGE and MAgPIE can be explained by variations in management and crop types (e.g. whether the LUMs assume C3 or C4 crops to be grown in certain regions), and the area and location of managed land, which differs considerably by the end of the century, especially in Africa (Fig. 2a). Sensitivity simulations in which N fertilizer rates, cropland area, atmospheric CO_2 mixing ratio, or the dynamic PHU calculation (i.e. adaption to climate change via selecting suitable varieties, see Sect. 2.1) were fixed at year 2009 levels indicate that around 62% and 39% (IMAGE and MAgPIE) of the crop production increase in the BASE simulations can be attributed to increases in N fertilizer rates, 22% and 74% to cropland expansion, 26% and 10% to increased atmospheric CO_2 levels, and 9% and 4% to dynamic PHU calculation (Fig. A4a). The numbers do not add up to 100% due to non-linear effects, interdependencies between variables (crop area/fertilization) and additional influences (climate, N deposition, crop types and irrigation) we did not analyse.

Crop production calculated with LPJ-GUESS is reduced in all mitigation simulations compared to BASE, by contrast to a set requirement in the LUMs to retain annual production at similar levels to BASE: In the LUMs this is achieved through further technology increases compared to BASE. The decline simulated in LPJ-GUESS, which is larger for MAgPIE than for IMAGE, especially for ADAFF (IMAGE -3% for the 2090-2099 period compared to 2090-2099 BASE; MagPIE -35%), occurs because in LPJ-GUESS we capture only yield increases achieved through higher N input, and thus only cover part of the additional technological yield increase assumed by the LUMs for the mitigation scenarios (and which thus allows for shrinking production area, see Table A2).

3.6 Nitrogen loss

Global N loss in the BASE simulations increases strongly over the 21st century by 82% for IMAGE and 62% for MAgPIE (Fig. 3a). Most of the increase is caused by fertilization but increasing N deposition (+19% over the century) contributes as well. N loss is higher for MAgPIE than for IMAGE at the beginning and end of the 21st century, but higher for IMAGE around mid-century (Table 1, Fig. A1j). As total fertilizer application is higher for MAgPIE throughout the entire century these differences can be explained by spatial heterogeneity (e.g. in India where fertilization has a large impact on N loss, fertilizer rates are generally higher for IMAGE than for MAgPIE). Increases in N losses correspond roughly to increases in N application, and to crop production increases in the original LUMs, indicating that crops in LPJ-GUESS approach N saturation, and cannot use the additional N for higher yields. Sensitivity simulations indicate that most of the N loss increase between 2000-2009 and 2090-2099 is induced by increased fertilizer application/cropland expansions, while increasing atmospheric CO_2 and dynamic PHU calculation reduce N loss (Fig. A4b).

N loss in ADAFF decreases by 6.7% for IMAGE and 13.2% for MAgPIE compared to BASE 2090-2099 (Fig. 3b), but with large variability across regions (Fig. 4b). The decrease can be attributed to lower global fertilizer amounts in ADAFF than in BASE for both LUMs, as forests are not fertilized. In the BECCS simulations the decrease is larger for IMAGE (-10.3%) than for MAgPIE (-7.6%), including substantial regional variations, especially in South America (Fig. 4c). The fertilization of bioenergy crops (for which low fertilizer rates are assumed in the LUMs) adds N to the system, however, crop N uptake and subsequent removal during harvest are also enhanced, resulting in a net N removal (and thus less N available to leave the system via leaching or in gaseous form). N loss reductions in BECCS-ADAFF lie between ADAFF and BECCS for MAgPIE (-9.2%) but are smallest amongst all mitigation simulations for IMAGE (-5.5%).

3.7 BVOCs

Changes in BVOC emissions are dominated by isoprene emissions, which are, by weight, an order of magnitude higher than those of monoterpenes (Table 1, Fig. A1k-l). In the BASE simulations, total BVOC emissions from 2000-2009 to 2090-2099 decrease by 11% for IMAGE LU but only by 2% for MAgPIE LU (Fig. 3a). Spatially, BVOC emissions generally increase

in high latitudes but decrease in the tropics (Fig. 4a), corresponding to northwards forest shifts and deforestation/forest degradation concentrated in low latitudes (not shown). The tropics dominate the overall response due to much higher typical emission rates.

As expected from the generally high emission potential of woody vegetation (compared with herbaceous), BVOC emissions increase in the ADAFF simulations (24% and 16% for IMAGE, respectively MAgPIE). Following the spatial change in forest cover, the increase mainly occurs in the tropics (Fig. 4b). In the BECCS simulations, BVOC emissions decrease by 8% for IMAGE and by 2% for MAgPIE (Fig. 3c) due to the low emissions of grassy bioenergy crops (corn). BECCS-ADAFF results in 11% and 7% higher emissions for IMAGE, respectively MAgPIE (Fig. 3d).

4 Discussion

Our analysed ES indicators can serve as proxies for several ES linked to human well-being. Table 2 gives a qualitative overview how these ES indicators and corresponding ES are interlinked. We do not aim to value and rank individual ES indicators and thus do not assess here how relative changes could be differently prioritized in decision-making for land management. While this is certainly a too simple generalization for fully assessing the implications of such scenarios, ranking or prioritizing individual ES indicators is a substantial challenge, which is beyond the scope of this study. A given relative change can be more crucial for some indicators than for others and their importance can also vary across regions. The changes in our mitigation simulations will occur in addition to the changes originating from climate change, increased atmospheric CO_2, and non-mitigation related LU/management changes over this century, thereby intensifying or dampening the supply of ES to human societies.

4.1 Climate regulation via biogeochemical and biophysical effects

In our LPJ-GUESS simulations, the IMAGE mitigation scenarios are slightly more effective than the MAgPIE scenarios in terms of simulated C uptake, but all simulations diverge from the CDR target implemented in the LUMs (see Sect. 4.2). Land-based mitigation might also impact the emissions of other GHG (e.g. N_2O, see Table 2), but future fertilizer application rates and emissions from bioenergy crops are highly uncertain (Davidson and Kanter, 2014). While N_2O contributes to global warming, the net effect of reactive N might be a cooling when accounting for short-lived pollutants and interactions with the C cycle (Erisman et al., 2011). In our LPJ-GUESS simulations, reductions in N losses suggest a decrease in gaseous N emissions for both ADAFF and BECCS, however, no quantifications are possible as LPJ-GUESS does not yet differentiate between different forms of N losses.

Biogeosciences Discuss., doi:10.5194/bg-2017-160, 2017
Manuscript under review for journal Biogeosciences
Discussion started: 19 May 2017

Climate effects of well-mixed GHG are global, whereas biophysical effects are primarily felt on the local scale (Alkama and Cescatti, 2016). Surface albedo in regions with seasonal snow cover is expected to decrease significantly for afforestation scenarios (Bala et al., 2007;Bathiany et al., 2010;Betts, 2000;Davies-Barnard et al., 2014), thereby opposing the biogeochemical cooling effect. Effects of enhanced forest cover are less pronounced in lower latitudes (Li et al., 2015) and for BECCS scenarios (Smith et al., 2016). Limited impacts of BECCS on albedo also emerge in our simulations. However, we find noticeable albedo reductions in ADAFF despite the fact that for both LUMs afforestation was concentrated in snow-free regions where satellites rarely observe albedo differences between forests and open land exceeding 0.05 (Li et al., 2015).

High evapotranspiration rates, as often observed in forests, cool the local surface. In tropical regions, this cooling effect exceeds the warming effect from lower albedo (Alkama and Cescatti, 2016;Li et al., 2015). In our simulations, impacts of land-based mitigation on global evapotranspiration range from -0.4% (IMAGE BECCS) to +2.1% (IMAGE ADAFF). On the regional scale this can translate to absolute changes of more than 100 mm yr^{-1} in some tropical areas (e.g. central Africa). While these changes seem relatively small compared to the mean differences between forests and non-forests reported by Li et al. (2015) (141 mm yr^{-1} 20°N-50°N, 238 mm yr^{-1} 20°S-50°S, 428 mm yr^{-1} 20°S-20°N), our results still suggest that Reducing Emissions from Deforestation and Forest Degradation (REDD) activities would not only help mitigating global climate change via avoided C losses but could provide additional local cooling, serving as a "payback" for tropical countries. The simulated evaporative water loss due to ADAFF at the end of the century (~1200 km^3 yr^{-1} for IMAGE, 750 km^3 yr^{-1} for MAgPIE for a C sequestration rate of ~0.8 and 1.4 GtC yr^{-1}, respectively) is higher than estimated by Smith et al. (2016) (370 km^3 yr^{-1} for a C sequestration rate of ~1.1 GtC yr^{-1}). Furthermore, Smith et al. (2016) assumed that dedicated rain-fed bioenergy crops consume more water than the replaced vegetation (with additional water required for CCS), while in our simulations bioenergy crops had little impact on evapotranspiration as they were represented as corn. LU driven changes in evapotranspiration rates can also modify the amount of atmospheric water vapour and cloud cover, with consequences for direct radiative forcing, planetary albedo and precipitation (e.g. Sampaio et al., 2007, see also Table 2), however, such interactions cannot be captured by our model setup.

BVOCs influence climate via their influence on tropospheric ozone, methane and secondary organic aerosol formation (Arneth et al., 2010;Scott et al., 2014), which depend strongly on local conditions such as levels of nitrogen oxides (NO_X) or background aerosol (Carslaw et al., 2010;Rosenkranz et al., 2015). While enhanced leaf level BVOC emissions are driven by warmer temperatures, uncertainties arise from additional CO_2 effects (which suppress leaf emissions). On the canopy scale, isoprene emissions generally decrease for deforestation scenarios (Hantson et al., 2017) but increase for woody biofuel plantations, which tend to use high-emitting tree species (Rosenkranz *et al.*, 2015). In our simulations, we find increases in BVOC emissions for ADAFF but not so for BECCS as bioenergy crops are grown as low-emitting corn. The high spatial and temporal variability of the BVOC emissions, complications of atmospheric transport and gaps in our knowledge of the reactions involved make it difficult to judge if an increase in BVOC emissions results in a warming or cooling. The global

effect (assuming present-day air pollution in 1850 and excluding aerosol-cloud interactions) of historic (1850s-2000s) reductions in BVOC emissions (20-25%) due to deforestation has been estimated to be a cooling of -0.11 ± 0.17 W m^{-2} (Unger, 2014). Accordingly, the substantial increase in BVOC emissions in our ADAFF simulations (16% and 24%) might induce a similar warming.

4.2 Carbon uptake in LPJ-GUESS

C uptake in the three land-based mitigation options in LPJ-GUESS is lower than the target value used in the LUMs. When the underlying reasons for model-model discrepancies are explored, a number of reasons can be identified such as bioenergy yields, forest regrowth, legacy effects from past LUC and recovery of soil carbon in response to reforestation. Additionally, in the BECCS scenarios, the CDR target was implemented as a CCS target which does not account for additional LUC emissions, partly explaining the lower CDR values.

For forest regrowth, the current model configuration of LPJ-GUESS simulates natural forest succession, including the representation of different age classes. Krause et al. (2016) showed that the recovery of C in ecosystems following different agricultural LU histories broadly agreed with site-based measurements. LPJ-GUESS also has N (and soil water availability) as an explicit constraint on forest growth and has been successfully tested against a broad range of observations (Fleischer et al., 2015;Smith et al., 2014). While these studies indicate an overall realistic rate of forest growth the model output has not yet been systematically assessed against fast-growing monoculture plantations that are used in some reforestation/afforestation projects. Forest (re)growth is simulated very differently in LPJ-GUESS (representing different age classes and their competition), IMAGE-LPJmL (one individual per PFT) and MAgPIE-LPJmL (managed regrowth, see Sect. 2.2). LPJmL also does not yet consider N constraints on vegetation regrowth. C losses from deforestation and maximum C sequestration following reforestation depend on potential C densities which are likely different in LPJmL and LPJ-GUESS. In the LUMs, the model's algorithm knows C pools and can thus decide to reforest the most suitable areas while in LPJ-GUESS other regions might have more reforestation potential. Additionally, in MAgPIE, climate change impacts on natural vegetation C stocks have not been accounted for in the CDR target. In IMAGE, reforestation preferentially occurs in degraded forests which are assumed to be completely deforested. While we follow this approach in LPJ-GUESS to ensure consistency, C accumulation potential in these areas is likely overestimated as some tree cover is likely to exist in degraded forests. Finally, soil C sequestration rates are likely different between LPJ-GUESS and LPJmL, especially for MAgPIE-LPJmL where the assumption of soil C recovering within 20 years is likely overoptimistic (see Krause *et al.*, 2016).

For BECCS, LPJ-GUESS simulates CCS rates of ~2.2 and 1.8 GtC yr^{-1} (IMAGE and MAgPIE) by the end of the 21st century, compared to ~2.8 GtC yr^{-1} reported from the LUMs directly. The number from the LUMs is close to the mean removal rate of 3.3 GtC yr^{-1} reported in Smith et al. (2016) for scenarios of similar production area (380-700 vs.

493/363 Mha in our IMAGE/MAgPIE BECCS scenario) and slightly larger CO_2 mixing ratios (430-480 ppmv vs. 424 ppmv). Discrepancies between the models arise mainly from differences in assumptions about bioenergy crop yields. In our LPJ-GUESS simulations we grew bioenergy crops as a crop functional type with parameters taken to represent maize/corn. By the end of the century, bioenergy yields simulated by LPJ-GUESS are higher for MAgPIE BECCS LU patterns (on average 13.8 t dry mass ha^{-1} yr^{-1}, 10% of total above-ground biomass remaining onsite) than for IMAGE BECCS LU patterns (12.2 t dry mass ha^{-1} yr^{-1}) due to different fertilizer rates and production locations. Bioenergy crop yields in LPJ-GUESS might be influenced by inconsistencies between the models about fertilization of bioenergy crops: While the LUMs generally assume high N application, fertilizer rates are reduced in areas used for bioenergy production because bioenergy crops are less N demanding. Consequently, the fertilizer rates from the LUMs might be insufficient to fulfil the N demand of bioenergy crops in LPJ-GUESS where corn yields respond strongly to fertilization (Blanke et al., 2017). In contrast, bioenergy crops in the LUMs are represented by dedicated lignocellulosic energy grasses. Reported yields of dedicated bioenergy crops under present-day conditions show large variability (miscanthus x giganteus: 5-44 t dry mass ha^{-1} yr^{-1}; switchgrass: 1-35 t ha^{-1} yr^{-1}; woody species: 0-51 t ha^{-1} yr^{-1}), depending on location, plot size and management (Searle and Malins, 2014). By the end of the century, the LUMs report average bioenergy yields of ~15.0 t ha^{-1} yr^{-1} (IMAGE) and ~20.3 t ha^{-1} yr^{-1} (MAgPIE), but how bioenergy yields will evolve in reality when averaged across regions (including more marginal land) is highly uncertain (Creutzig, 2016;Searle and Malins, 2014;Slade et al., 2014).

Legacy effects from historic LU might also impact future C uptake as the soil C balance continues to respond to LUC decades or even centuries after (Krause et al., 2016;Pugh et al., 2015). We assessed the contribution of legacy effects by comparing a LPJ-GUESS simulation in which LU (but not climate and CO_2) was held constant from year 1970 for IMAGE and 1995 for MAgPIE (consistent with the scenario starting years in each model) with a run with fixed LU from year 1901 on. The differences then seen over the 21st century between these two simulations would arise chiefly from legacy fluxes of 20th century LUC. These were found to be ~17-18 GtC (not shown), accounting for part of the difference in uptake between LPJ-GUESS and the LUMs. In the LUMs, harmonisation to history has been done with respect to land cover, but not with respect to changes in vegetation and soil C pools (prior to 1970/1995).

Our results show that assumptions about forest growth and C densities, bioenergy crop yields, and time scales of soil processes can critically influence the C removal potential of land-based mitigation. Large uncertainties about forest regrowth trajectories in different DGVMs (Pongratz et al., in preparation) and BECCS potential to remove C from the atmosphere (Creutzig et al., 2015;Kemper, 2015) have been reported before, including the importance of second-generation bioenergy crops (Kato and Yamagata, 2014) and LU-driven C losses in vegetation and soils (Wiltshire and Davies-Barnard, 2015). This is clearly an important subject for future research. Additional analyses about the difference in C removal between the LUMs and LPJ-GUESS, including results from additional DGVMs, are on-going and will be published in a separate manuscript (Krause et al., in preparation).

Biogeosciences Discuss., doi:10.5194/bg-2017-160, 2017
Manuscript under review for journal Biogeosciences
Discussion started: 19 May 2017

4.3 Water availability

Forests generally reduce local river flow compared to grass- and croplands. Based on 26 catchment data sets including 504 observations worldwide, Farley et al. (2005) reported an average decrease of 44% and 31% in annual stream flow caused by woody plantations replacing grasslands, respectively shrublands, with large variability across different plantation ages. The reduction in global annual runoff due to ADAFF (1200/600 km^3 yr^{-1} compared to BASE 2090-2099) corresponds to around 16-32% of human runoff withdrawal (Oki and Kanae, 2006), which could be seen as a potential risk to freshwater supply. Regional changes range from -5.2% to +0.4% across all scenarios, but in many cases impacts on irrigation (the largest consumer of freshwater) potential in fact might be small: Modelling work suggests that renewable water supply will exceed the irrigation demand in most regions by the end of the century for RCP8.5 (Elliott et al., 2014). However, Elliott et al. also found that regions with the largest potential for yield increases from increased irrigation are also the regions most likely to suffer from water limitations. Patterns will be different in an RCP2.6 world as CO_2 fertilization significantly reduced global irrigation demand (8-15% on presently irrigated area) in the Elliott et al. crop models and climate impacts are expected to be less severe in RCP2.6.

In uncoupled simulations, such as done here, atmospheric feedbacks related to higher evapotranspiration cannot be captured. At regional/continental scale, there is evidence that afforestation might actually increase runoff as the larger evapotranspiration rates enhance precipitation (Ellison et al., 2012). However, based on regional climate modelling, Jackson et al. (2005) concluded that atmospheric feedbacks would unlikely offset water losses in temperate regions where the additional atmospheric moisture cannot be lifted high enough to form clouds.

Changing runoff affects water supply but can also contribute to changes in flood risks. Bradshaw et al. (2007), using a multi-model approach and data from 56 developing countries, calculated a 4-28% increase in flood frequency and a 4-8% increase in flood duration for a hypothetical reduction of 10% natural forest cover, while e.g. van Dijk et al. (2009) questioned forest potential to reduce large-scale flooding and argued that the frequency of reported floods can be mainly explained by population density. Ferreira and Ghimire (2012) extended the original Bradshaw sample to all counties (129) that reported at least one large flood between 1990 and 2009 and included socioeconomic factors in their analyses. They found no longer a statistically significant correlation between forest cover and reported floods. In our simulations, peak monthly runoff is generally reduced for ADAFF, however, given maximum regional changes of -3.6% (Africa, IMAGE ADAFF) and presuming that floods are largely controlled by other factors than forest cover, we expect large-scale LU effects on flooding to be limited.

Biogeosciences Discuss., doi:10.5194/bg-2017-160, 2017
Manuscript under review for journal Biogeosciences
Discussion started: 19 May 2017

4.4 Food production

Increasing food production in a sustainable way to feed a growing population is a major challenge of the modern world (Tilman et al., 2002). Population and income growth (in SSP2 population peaks in 2070 at 9.4 billion people, and per capita GDP continuous to increase until 2100 (Dellink et al., 2017;Samir and Lutz, 2017)) will be accompanied by an increased need of total calories and shifts in diets. For SSP2, economic modelling suggests that global food crop demand will increase by 50-97% between 2005 and 2050 (Valin et al., 2014). In the present study, the corresponding increase reported directly from the LUMs is 38% for IMAGE and 52% for MAgPIE (78% and 96% in year 2100), equivalent to a 21% and 7% increase in per-capita food crop supply. In our LPJ-GUESS BASE simulations we find crop production increases of ~22/45% (IMAGE/MAgPIE) by 2050 and ~24/64% by the end of the century (corresponding to a per-capita increase for MAgPIE but a decrease for IMAGE). However, the production increase is significantly reduced in the mitigation simulations, especially for MAgPIE ADAFF due to production shifts and the abandonment of croplands for reforestation. Crop yields in LPJ-GUESS are a function of environmental conditions, fertilizers, irrigation, and adaption to climate change by selecting suitable varieties. In our BASE simulations, the combined effect is an average yield increase of ~17% and ~41% (IMAGE and MAgPIE) between 2000-2009 and 2090-2099. In the LUMs the mitigation scenarios are characterized by additional yield increases compared to BASE, triggered by increased land prices. This intensification is to some extent reflected in the fertilizer rates (derived from yields) provided by the LUMs, however, other management improvements and investments in research and development leading to higher-yielding varieties also impact future yield increases. Additional assumptions about yield increases driven by technological progress can thus not be captured by LPJ-GUESS. The simulated decline in productivity in response to shrinking cropland area in the mitigation scenarios suggests that, when adapting N fertilization, irrigation and cropland area and location from the LUMs, additional yield increases of up to 6.6% and 35% (IMAGE and MAgPIE) would be required between the 2000s and the 2090s to produce the same amount of food crops as in the BASE scenario, equivalent to ~0.07% and 0.33% per year.

4.5 Water and air quality

Managed agricultural systems directly impact freshwater quality. Historically, approximately 20% of reactive N moved into aquatic ecosystems (Galloway et al., 2004), causing drinking water pollution and eutrophication. The global N-leaching rate is highly uncertain but the rate simulated with LPJ-GUESS (if all N losses are assumed to be via leaching) is within the range of published studies (Olin et al., 2015a). As N loss in LPJ-GUESS is largely driven by fertilization (Blanke et al., 2017), the much higher future fertilization rates compared to present-day (+78% for IMAGE; +95% for MAgPIE) lead to an increase in N loss of ~82% and 62% in BASE. Such a massive increase would have severe impacts on water ways and coastal zones, where current levels of N pollution are already having substantial effects (Camargo and Alonso, 2006). In contrast to the BASE simulations, the mitigation simulations result in somewhat lower N losses because less fertilizer is

applied (ADAFF) or because bioenergy harvest removes more N than added via bioenergy crop fertilization (BECCS). Simulated N losses in LPJ-GUESS are affected by different assumptions about N fertilizers and inconsistencies between the models: Fertilizer rates in the LUMs were calculated to support the estimated crop yields (and hence the ensuing N demand). The resulting grid-cell averages available to LPJ-GUESS did not take into account differences in N application across crop types in a grid-cell (Mueller et al., 2012). Additionally, IMAGE and MAgPIE simulate further increases in crop productivity and N use efficiency and therefore nutrient recovery in harvested biomass, which may only be partly captured by LPJ-GUESS (see Sect. 4.4).

Although we do not explicitly simulate emissions of N gases, increased N losses suggest an excess of soil N, which increases the likelihood of gaseous reactive N emissions such as NO_X and ammonia (NH_3) pollution, contributing to particulate matter formation, visibility degradation and atmospheric N deposition (Behera et al., 2013). The chemical form and level of these emissions will strongly depend on soil water status (Liu et al., 2007). Improvements in air quality, e.g. via reductions in tropospheric ozone (O_3), are not only relevant for human health but can also enhance plant productivity and crop yields (Wilkinson et al., 2012). The response of O_3 to BVOC emissions changes depends on the local NO_X:BVOC ratio (Sillman, 1999). An increase in BVOC emissions slightly suppresses O_3 concentration in remote regions but promotes it in regions of high NO_X background (Pyle et al., 2011). Ganzeveld et al. (2010) used a chemistry-climate model to study the effects of LUC in the SRES A2 scenario (tropical deforestation) on atmospheric chemistry. By year 2050, they found increases in boundary layer ozone mixing ratios of up to 9 ppb (20%). Changes in the concentration of the hydroxyl radical resulting from deforestation (the primary atmospheric oxidant, and main determinant of atmospheric methane lifetime) are much less clear due to uncertainties in isoprene oxidation chemistry (Fuchs et al., 2013;Hansen et al., 2017;Lelieveld et al., 2008), but O_3 concentrations were not sensitive to this uncertainty (Pugh et al., 2010). ADAFF describes a reverse scenario, with forest expansion being largely concentrated in the tropics. The sign of changes in the ADAFF simulations is reverse to changes in Ganzeveld et al.: By mid-century, global N loss in ADAFF decreases by ~8% and 4% and isoprene emissions increase by ~14% and 4% compared to BASE. Consequently, we would expect tropospheric O_3 burden in ADAFF to decrease in the tropics but to increase in large parts of the mid-latitudes. However, changes in overall air quality will likely be dominated by anthropogenic emissions rather than LUC (Martin et al., 2015). BVOC emissions might also increase in bioenergy scenarios (Rosenkranz *et al.*, 2015), however, this does not happen in our study as the LUMs assumed grasses to be the predominant bioenergy crop.

4.6 Potential impacts on biodiversity

Global-scale approaches that link changes in LU, climate and other drivers to effects on biodiversity are scarce, and burdened with high uncertainty, though some approaches exist (Alkemade et al., 2009;Visconti et al., 2011) and biodiversity,

whether it is being perceived as a requisite for the provision of ES or an ES per se, with its own intrinsic value (Liang et al., 2016;Mace et al., 2012), has not been considered in our analysis.

Nevertheless, it is evident that biodiversity can be in critical conflict with demands for land resources such as food or timber (Behrman et al., 2015;Murphy and Romanuk, 2014). LUC has been the most critical driver of recent species loss (Jantz et al., 2015;Newbold et al., 2014). This has led to substantial concerns that land requirements for bioenergy crops would be competing with conservation areas directly or by leakage. Santangeli et al. (2016) found around half of today's global bioenergy production potential to be located either in already protected areas or in land that has highest priority for protection, indicating a high risk for biodiversity in absence of strong regulatory conservation efforts.

In principle, avoided deforestation and reforestation/afforestation should maintain and enhance habitat and species richness, since forests are amongst the most diverse ecosystems (Liang et al., 2016). Forestation could also support the restoration of degraded ecosystems. However, success of large-scale reforestation/afforestation programs under a C-uptake as well as a biodiversity perspective will depend critically on the types of forests promoted and so far show mixed results (Cunningham et al., 2015;Hua et al., 2016). Likewise, even under a globally implemented forest conservation scheme there may be cropland expansion into non-forested regions that could well be C-rich (implying reduced overall C-mitigation) but also diverse such as savannas or natural grasslands.

4.7 Conclusions

Terrestrial ecosystems provide us with many valuable services like climate and air quality regulation, water and food provision, or flood protection. Land-based mitigation in LPJ-GUESS substantially affected simulated ecosystem functions. In all mitigation simulations, what might generally be perceived as beneficial effects on some ecosystem functions and their services, were counteracted by negative effects on others, including substantial regional variations. Environmental side-effects in our ADAFF simulations were usually larger than in BECCS even though the achieved C removal was similar (IMAGE) or lower (MAgPIE).

Policy makers should be aware of manifold side effects - be they positive or negative - when discussing and evaluating the feasibility and effects of different climate mitigation options, possibly involving the prioritization of individual ES at the costs of exacerbating other challenges. Our analysis makes some of these trade-offs explicit, but there are many other services offered by ecosystems much more difficult to quantify, particularly relating to cultural service, which also need to be considered. Any discussion about land-based climate mitigation efforts should take into account their effects on ES beyond climate in order to avoid unintended negative consequences, which would be both intrinsically undesirable and may also affect the effective delivery of climate mitigation through societal feedbacks.

Biogeosciences Discuss., doi:10.5194/bg-2017-160, 2017
Manuscript under review for journal Biogeosciences
Discussion started: 19 May 2017

Tables and Figures

Table 1: Global net-total values ± standard deviations (over 10 years) of all analysed ecosystem functions as simulated by LPJ-GUESS for all scenarios and different time-periods and for IMAGE LU patterns (blue) and MAgPIE LU scenarios (red). Total C is the sum of vegetation C, soil C, product C (wood removed during deforestation but not immediately oxidized) and cumulative CCS.

Ecosystem function	BASE		ADAFF	BECCS-ADAFF	BECCS
	2000-2009	2090-2099			
Vegetation C [GtC]	380 ± 1 393 ± 2	415 ± 2 459 ± 2	478 ± 4 496 ± 5	444 ± 3 476 ± 3	391± 2 450 ± 2
Soil and litter C [GtC]	1575 ± 1 1585 ± 1	1578 ± 1 1587 ± 1	1588 ± 1 1599 ± 2	1580 ± 1 1592 ± 2	1567 ± 1 1583 ± 1
Product C [GtC]	5.7 ± 0.4 4.6 ± 0.2	1.5 ± 0.1 0.3 ± 0.0	0.4 ± 0.0 0.4 ± 0.0	1.0 ± 0.1 0.3 ± 0.0	2.4 ± 0.2 0.6 ± 0.1
Cumulative CCS [GtC]	- -	- -	- -	52.1 ± 3.4 34.7 ± 2.5	100.0 ± 6.6 73.5 ± 5.6
Total C [GtC]	1961 ± 2 1983 ± 2	1995 ± 3 2047 ± 3	2067 ± 5 2096 ± 7	2077 ± 7 2103 ± 7	2060 ± 7 2108 ± 8
January albedo	0.250 ± 0.004 0.249 ± 0.004	0.240 ± 0.002 0.240 ± 0.002	0.237 ± 0.002 0.238 ± 0.002	0.238 ± 0.002 0.240 ± 0.002	0.241 ± 0.002 0.240 ± 0.002
July albedo	0.182 ± 0.001 0.182 ± 0.001	0.179 ± 0.001 0.179 ± 0.001	0.177 ± 0.001 0.177 ± 0.001	0.178 ± 0.001 0.178 ± 0.001	0.180 ± 0.001 0.179 ± 0.001
Evapotranspiration [1000 km^3 yr^{-1*}]	58.6 ± 0.7 58.9 ± 0.7	57.9 ± 1.2 58.8 ± 1.2	59.1 ± 1.2 59.5 ± 1.2	58.6 ± 1.2 59.3 ± 1.2	57.7 ± 1.2 58.9 ± 1.2
Annual runoff [1000 km^3 yr^{-1}]	52.5 ± 3.1 52.2 ± 3.1	55.1 ± 2.8 54.3 ± 2.8	53.9 ± 2.8 53.7 ± 2.8	54.4 ± 2.8 53.9 ± 2.8	55.3 ± 2.8 54.2 ± 2.8
Peak monthly runoff [1000 km^3 $month^{-1}$]	17.9 ± 1.0 17.9 ± 1.0	18.9 ± 1.2 18.8 ± 1.2	18.7 ± 1.2 18.6 ± 1.2	18.8 ± 1.2 18.7 ± 1.2	19.0 ± 1.2 18.8 ± 1.2
Crop production [Ecal]	28.9 ± 0.5 27.5 ± 0.9	35.9 ± 0.5 45.2 ± 0.4	34.7 ± 0.5 29.3 ± 2.0	34.0 ± 0.5 35.5 ± 0.7	33.5 ± 0.5 40.8 ± 0.5
N loss [TgN yr^{-1}]	60.3 ± 7.1 73.3 ± 6.8	109.7± 13.2 119.0 ± 8.0	102.3 ± 12.5 103.2 ± 8.4	103.6 ± 12.3 108.1 ± 7.9	98.4 ± 11.5 110.0 ± 7.0
Isoprene emissions [TgC yr^{-1}]	477 ± 8 503 ± 9	419 ± 9 495 ± 10	529 ± 11 578 ± 13	469 ± 10 532 ± 11	382 ± 8 483 ± 10
Monoterpene emissions [TgC yr^{-1}]	40.7 ± 0.6 41.9 ± 0.7	38.9 ± 0.9 40.5 ± 0.9	40.2 ± 1.0 41.6 ± 1.0	39.4 ± 0.9 40.9 ± 0.9	38.2 ± 0.9 40.4 ± 0.9

*1000 km^3 are equal to 1 Eg of water

Biogeosciences Discuss., doi:10.5194/bg-2017-160, 2017
Manuscript under review for journal Biogeosciences
Discussion started: 19 May 2017

Table 2: Overview over how changes in ecosystem functions analyzed in this study (which can serve as proxies for a range of ecosystem services, ES) could be interpreted. An increase in an ecosystem function can be positive (+), negative (-), zero (0) or either positive or negative (+/-), depending on the background conditions or perspective. Effects can be small (+ or -) or large (++ or --). Regional effects are shown without brackets and global effects, where relevant, in brackets. Indirect effects that are more directly represented by another ecosystem function considered here are not shown. The table is based on evidence from the literature in cases the link is not directly clear (see footnotes).

Ecosystem function	ES – climate change mitigation	ES – water availability	ES – flood protection	ES – water quality	ES – air quality	ES – food production
C storage ↑	++ (++)					
Surface albedo ↑	++ (+)[a]					
Evapotranspiration ↑	++ (+/-)[b]					
Annual runoff ↑		++	-	0/+[c]		
Peak monthly runoff ↑		0/+[d]	--	0/-[e]		0/-[f]
Crop production ↑						++ (++)
N loss ↑	+/- (+/-)[g]			--[7]	- (-)[g]	
BVOC emissions ↑	+/- (+/-)[h]				0/-- (0/-)[i]	

Biogeosciences Discuss., doi:10.5194/bg-2017-160, 2017
Manuscript under review for journal Biogeosciences
Discussion started: 19 May 2017

[a] The global effects of LU-driven albedo changes seem to be small (e.g. de Noblet-Ducoudre et al., 2012).

[b] Local surface cooling as heat is needed to evaporate water. On larger scales, the effect could be either a warming due to increases in atmospheric water vapor (Boucher et al., 2004) or a cooling due to increased planetary albedo resulting from more cloudiness (Bala et al., 2007;Ban-Weiss et al., 2011).

[c] High flows imply more volume for dilution, prevent algae growth and maintain oxygen levels (Whitehead et al., 2009).

[d] Effect of peak monthly runoff on water availability is dependent on seasonal rainfall distribution and regional water storage capacity. Annual runoff is the clearer indicator.

[e] Soil erosion and associated re-mobilization of metals is enhanced during flood events (Whitehead et al., 2009).

[f] Due to flood damage in croplands (Posthumus et al., 2009).

[g] LPJ-GUESS at present calculates total N loss and does not differentiate between leaching and gaseous loss. As thus we indicate several effects that would arise from N emitted as N_2O (a greenhouse gas), emitted as NO_X or NH_3 (affecting air quality and aerosol formation), or as dissolved N. The net effect of N loss on climate has been estimated to be a small cooling (Erisman et al., 2011) but uncertainties are large.

[h] The net impact of BVOC emissions is very uncertain. On the global scale, increased BVOC emissions might result in a warming (Unger, 2014).

[i] BVOCs often increase ozone and aerosol formation, primarily locally (Rosenkranz et al., 2015), with principally opposite warming and cooling effects (Unger, 2014).

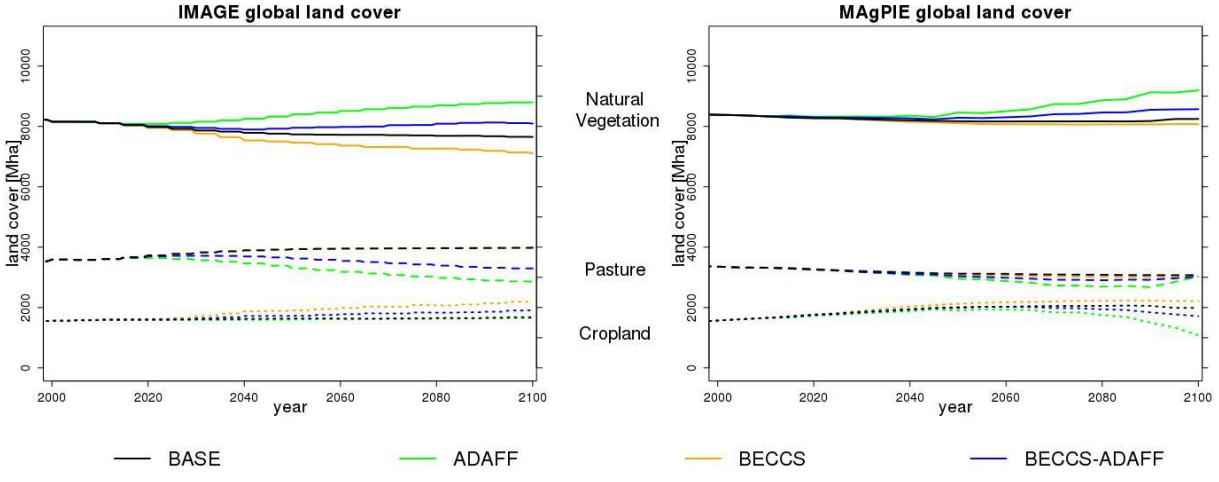

Figure 1: Time-series (2000-2100) of area under natural vegetation (including afforested area), pasture (including degraded forest area for IMAGE) and cropland (including bioenergy production area) for the different scenarios, for IMAGE (left) and MAgPIE (right).

Biogeosciences Discuss., doi:10.5194/bg-2017-160, 2017
Manuscript under review for journal Biogeosciences
Discussion started: 19 May 2017

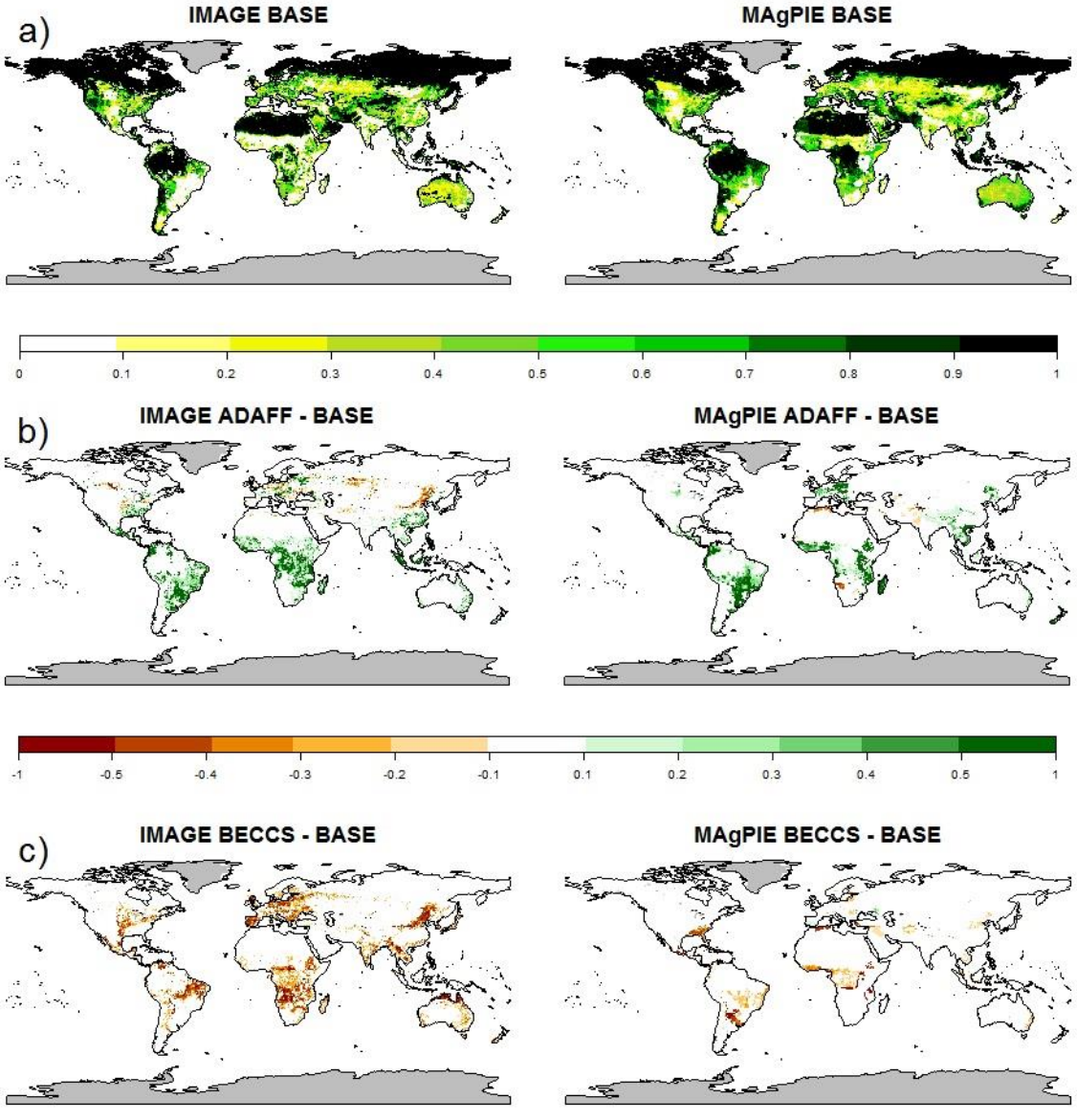

Figure 2: a) Fraction of grid-cell under natural vegetation (including afforested area but not degraded forests) by the end of the century (2090-2099) in the BASE scenario for IMAGE (left) and MAgPIE (right). b) Difference in the natural vegetation fraction between the ADAFF and the BASE scenario by the end of the century (2090-2099). c) Same as b) but between the BECCS and the BASE scenario.

Biogeosciences Discuss., doi:10.5194/bg-2017-160, 2017
Manuscript under review for journal Biogeosciences
Discussion started: 19 May 2017

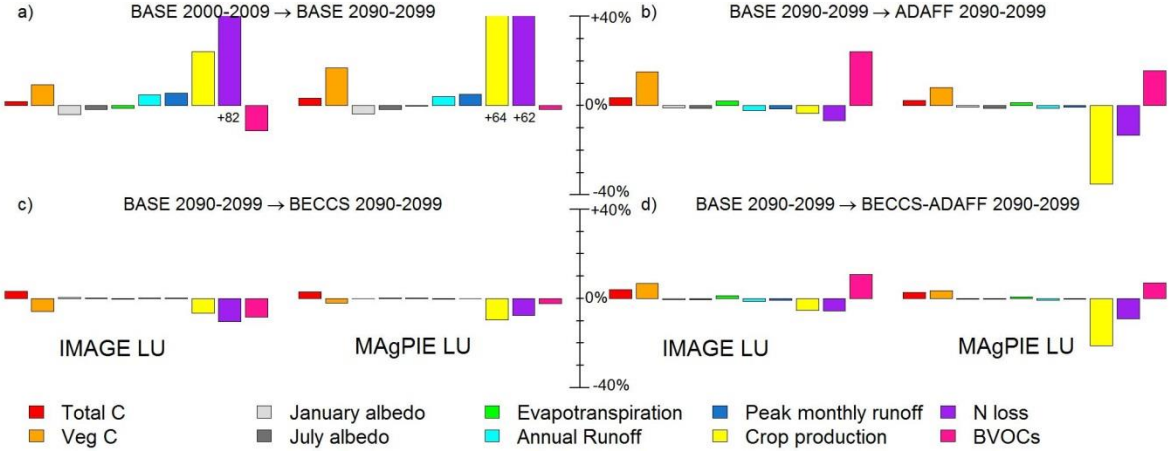

Figure 3: Global relative changes in analysed ecosystem functions simulated by LPJ-GUESS for different LU scenarios from IMAGE and MAgPIE. Changes are capped at ±40% for clarity reasons, values exceeding 40% are written below the bar. a) changes in the BASE simulation from 2000-2009 to 2090-2099. b) changes from BASE to ADAFF by the 2090-2099 period. c) same as b) but from BASE to BECCS. d) same as b) but from BASE to BECCS-ADAFF.

Biogeosciences Discuss., doi:10.5194/bg-2017-160, 2017
Manuscript under review for journal Biogeosciences
Discussion started: 19 May 2017

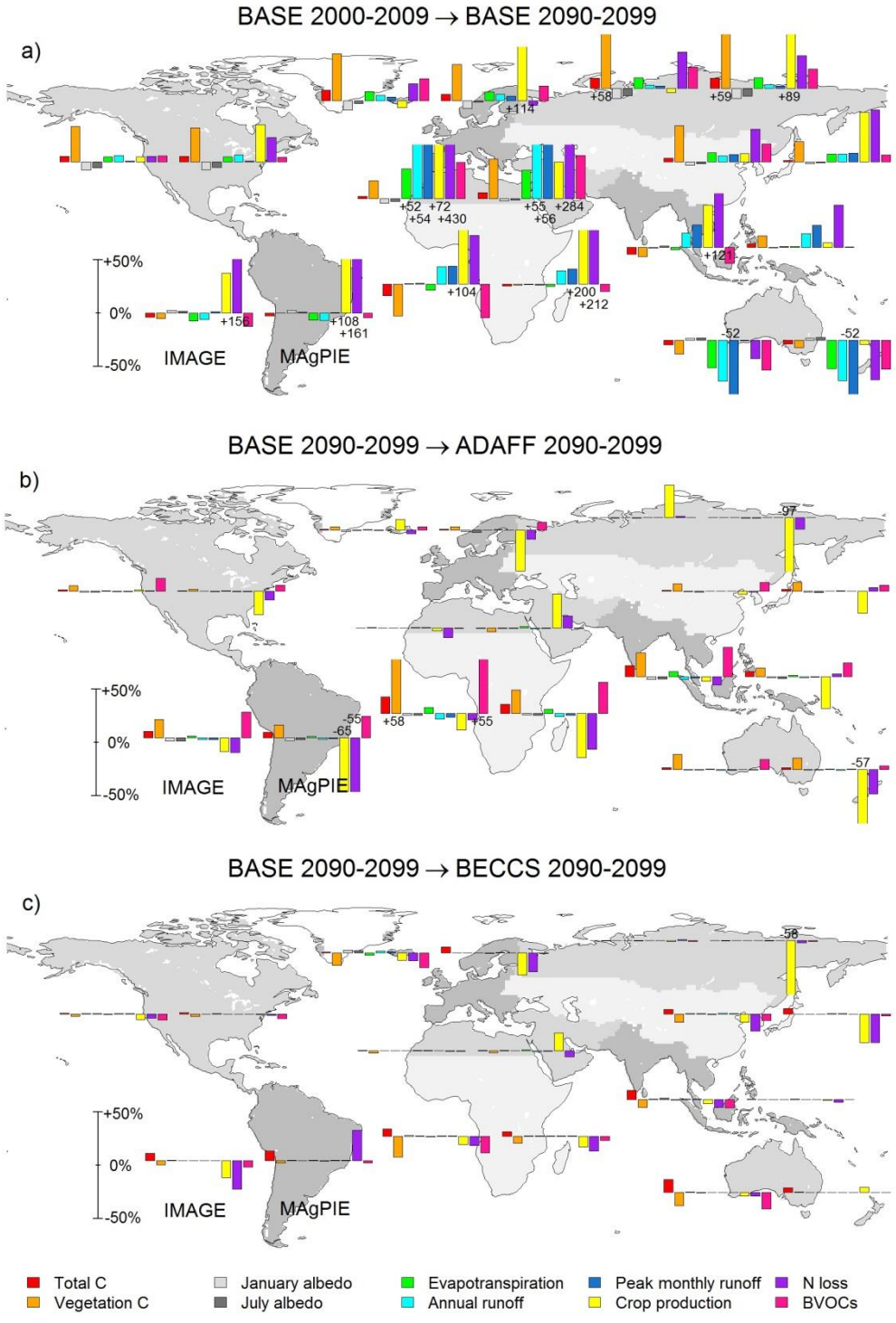

Biogeosciences Discuss., doi:10.5194/bg-2017-160, 2017
Manuscript under review for journal Biogeosciences
Discussion started: 19 May 2017

Figure 4: Regional relative changes in analysed ecosystem functions for IMAGE LU (left) and MAgPIE LU (right). Changes are capped at ±50% for clarity reasons, values exceeding ±50% are written upon/below the bar. Regions are aggregated Global Fire Emissions Database regions (Giglio et al., 2010) and are: North America, South America, Europe, Middle East, Africa, North Asia, Central Asia, South Asia, Oceania. a) changes in the BASE simulation from 2000-2009 to 2090-2099. b) changes from BASE to ADAFF by the 2090-2099 period. c) same as b) but from BASE to BECCS.

Data availability

Scientists interested in the LPJ-GUESS source code can contact the model developers (http://iis4.nateko.lu.se/lpj-guess/contact.html). Information about the land-use scenarios are avaiable from the IMAGE and MAgPIE groups (Jonathan.Doelman@pbl.nl; florian.humpenoeder@pik-potsdam.de). The LPJ-GUESS simulation data are stored at the IMK-IFU computing facilities and can be obtained on request (andreas.krause@kit.edu).

Appendix

A Conversion of IMAGE and MAgPIE land-use data to LPJ-GUESS input data

Land cover and crop transitions provided by the LUMs were converted to a suitable format to be used as input data for LPJ-GUESS simulations. Both LUMs provided the fraction of cropland (land used for food production and bioenergy production), pasture, forest, other natural land and built-up area in a 0.5° x 0.5° raster from 1901 to 2100, summing to one. Cropland and pasture land covers for LPJ-GUESS were directly adopted from the LUMs. On natural land, LPJ-GUESS simulates the dynamics of trees and grasses simultaneously as a function of environmental conditions, so the "forest" and "other natural" land covers were merged. IMAGE also uses a "degraded forest" land cover which is assumed to be completely deforested in IMAGE. To ensure consistency between the models we thus converted the corresponding fraction to pastures in LPJ-GUESS. Built-up area was negligible for all scenarios and for simplicity was also attributed to natural vegetation.

IMAGE used yearly (1970-2100) fractions of seven food crops (each separated into rain-fed and irrigated fractions) and rain-fed bioenergy grass in each grid-cell where cropland existed. MAgPIE provided yearly (1995-2100) fractions of 17 non-bioenergy crop types (separated into rain-fed and irrigated) and two rain-fed bioenergy crop types (grassy and woody). The attribution between LPJ-GUESS CFTs and LU-model crop types is shown in Table A1. For the years in which the LUMs did not provide CFT fractions (1901-1994 for MAgPIE and 1901-1969 for IMAGE) ratios were taken from the first provided year. We made the attribution to C3 or C4 grass in croplands based on a preceding pasture-only simulation which was forced by the same environmental conditions as our actual simulations (RCP2.6). Dedicated bioenergy crops are currently not

implemented in LPJ-GUESS and were represented by corn. Removed residues of bioenergy crops (90%) were included in the CCS calculation (see appendix B), while removed residues of food crops (75%) were emitted to the atmosphere. Residues left on-site (10% and 25%, respectively) went to the litter.

Average annual N fertilizer rates per cropland area (synthetic and organic fertilizer, derived from yields) were provided by IMAGE (1970-2100) and MAgPIE (1995-2100) and had to be extended to year 1901. Historic N fertilizer rates (synthetic fertilizer on C3+C4 annual and perennial crops) were available from the recently released LUH2 data set (Hurtt et al, in preparation, http://luh.umd.edu/index.shtml). However, as LUH2 only considers synthetic fertilizer, the correlation between LUH2 and the LUMs in the first provided year was poor in terms of spatial patterns and total amount of applied N, making a simple merging inapplicable. We thus decided to use IMAGE and MAgPIE N fertilizer rates and spatial patterns for the available time periods and computed a historic hindcast, starting with the initial spatial patterns and rates in IMAGE and MAgPIE multiplied by the relative year-to-year per-country change in the LUH2 data set in the period prior to 1970 and 1995, respectively. This resulted in a smooth historical to future N fertilizer dataset reflecting the LUMs spatial patterns in terms of absolute values with historic variations based on LUH2 relative changes and late historic to future variations adopted unmodified from the LUMs. Fertilizer rates differed significantly between IMAGE and MAgPIE, with MAgPIE exceeding IMAGE fertilizer rates in most locations. As no fertilization occurred before 1916 in LUH2 (before the Haber-Bosch process was found), we applied a minimum fertilizer rate of 6 kg N ha^{-1} yr^{-1} (in addition to atmospheric deposition) to all areas under crops throughout the entire simulation period to limit continued soil N depletion. As the LUMs only provided per-cropland fertilizer rates, we applied the same amount of fertilizer for all CFTs in a grid-cell, and distributed the annual amount over the year as a function of crop phenological state (Olin et al., 2015b).

B Carbon storage via CCS

Bioenergy yields included removed harvestable organs and crop residues (90% of total above-ground biomass). We estimated the total amount of C sequestered via CCS in the bioenergy simulations by assuming an 80% capture rate upon oxidization, which is the same value as in the LUMs (Klein et al., 2014). The total C was then the sum of terrestrial C (vegetation, soil and litter, C stored in wood products) and C stored via CCS.

C Albedo calculation

We calculated January and July surface albedo mainly based on mean winter (snow-free and snow-covered) and summer albedo values for different land cover types derived from MODIS satellite observations by Boisier et al. (2013). For the Southern Hemisphere we switched snow-free winter and summer albedo values. The LPJ-GUESS PFTs fractional plant cover determines the fraction of the grid-cell occupied by the land cover groups (crops, grasses, evergreen trees, deciduous trees, bare soil). For tropical evergreen trees we assumed an albedo of 0.140 year-round based on Boisier et al. (2013). For

woody bioenergy we assumed the same albedo as deciduous forests. The albedo of the non-vegetated fraction of the grid-cell under snow-free conditions was taken from Houldcroft et al. (2009) (average of white and black sky albedo), assuming a value of 0.15 at locations where no measurements were available. We estimated the grid-cell's monthly fraction under snow cover f_{snow} as

$$f_{\text{snow}} = \frac{z_{\text{sn}}}{0.01 + z_{\text{sn}}}$$

where z_{sn} is the average monthly snow depth (m) (Wang and Zeng, 2010, equation 17) which can be output from LPJ-GUESS. The albedo of the snow-covered fraction was calculated based on the values from Boisier et al. (2013) for snow-covered vegetation and bare soil and the grid-cell albedo was then the area-weighted average of snow-covered and snow-free albedos.

D Crop yield scaling

To account for spatial variations in crop management other than irrigation and fertilization, which are not accounted for in LPJ-GUESS, we scaled our food crop yields to the actual yields from the EarthStat data set (Monfreda et al., 2008), thereby only taking the absolute year-to-year changes from LPJ-GUESS. For this, we re-scaled yields of our four food CFTs (temperate wheat, temperate other summer crops, rice, corn) around the year 2000 (1997-2003) to match actual yields based on area-weighted yields of major food crops in the EarthStat data set (aggregated to 0.5° x 0.5° resolution; see Table A1 for which crop types were aggregated to which CFT). We then used these actual yields over the full crop yield time series, with year-to-year variations calculated based on the yield changes in LPJ-GUESS (area-weighted between rain-fed and irrigated yields). If crops were present in the LUMs but no adequate crop types were available in the EarthStat data set for a grid-cell we took the yields unmodified from LPJ-GUESS. We first converted dry matter yields per m^2 as given by LPJ-GUESS/EarthStat to fresh matter yields and finally to kcal. Fodder and cotton were not used for the crop production calculation. Total crop production was then the sum of temperate wheat, temperate other summer crops, rice and non-bioenergy corn production. Yields of bioenergy crops (grown as corn) were used unmodified to estimate CCS (see appendix B) due to limited observational data of bioenergy crop yields.

E BVOC emission factors of bioenergy crops

Crop BVOC emission scaling factors were taken from natural C3 or C4 grass, apart from woody bioenergy crops, which we grew as corn but used isoprene emission scaling factors of 45 μg(C) g^{-1}(leaf foliar mass) h^{-1} (Ashworth et al., 2012). These values are much higher than the values for normal grasses (8 μg g^{-1} h^{-1} for C4 grasses and 16 μg g^{-1} h^{-1} for C3 grasses) and account for the fact that isoprene emissions from typical woody bioenergy species like oil palm or willow are very high.

Biogeosciences Discuss., doi:10.5194/bg-2017-160, 2017
Manuscript under review for journal Biogeosciences
Discussion started: 19 May 2017

Table A1: Crop functional types (CFTs) used in this study, how the LU models' crop types were aggregated to these CFTs, and EarthStat major crops used to calculate circa year 2000 actual yields of these CFTs.

LPJ-GUESS CFT (photosynthetic pathway)	IMAGE and MAgPIE crop types aggregated to this CFT	EarthStat major crop types used to calculate circa year 2000 actual yields of LPJ-GUESS crops
temperate wheat (C3), representing C3 crops with winter or spring sowing depending on historical climate	temperate cereals, rapeseed	rye, barley, wheat, rapeseed
temperate other summer crops (C3) representing C3 crops with spring sowing only	potatoes, cassava, pulses, soybean, groundnuts, sunflower, palm oil, sugar beet, cotton, roots and tubers, oil crops, others	potato, cassava, groundnut, soybean, sunflower, oilpalm
rice (C3)	(paddy) rice	rice
corn (C4)	maize, tropical cereals, sugarcane, bioenergy crops	maize, millet, sorghum, sugarcane; bioenergy yields were not modified due to limited observational data
crop grass (C3 or C4)	fodder	unmodified as not used for crop production calculation

Table A2: Global area [Mha] under natural vegetation, pasture (brackets: degraded forests) and cropland (brackets: bioenergy) for the different scenarios for the 2000-2009 and 2090-2099 periods.

Scenario (year)	IMAGE			MAgPIE		
	Natural	Pasture	Cropland	Natural	Pasture	Cropland
BASE(2000-2009)	8155	3584(313)	1569	8367	3332	1609
BASE(2090-2099)	7664	3974(551)	1671	8225	3073	2010
ADAFF (2090-2099)	8783	2879(14)	1645	9139	2832	1338
BECCS (2090-2099)	7162	3981(551)	2165(493)	8074	3015	2219(363)
BECCS-ADAFF (2090-2099)	8119	3307(14)	1882(254)	8561	2964	1783(158)

Biogeosciences Discuss., doi:10.5194/bg-2017-160, 2017
Manuscript under review for journal Biogeosciences
Discussion started: 19 May 2017

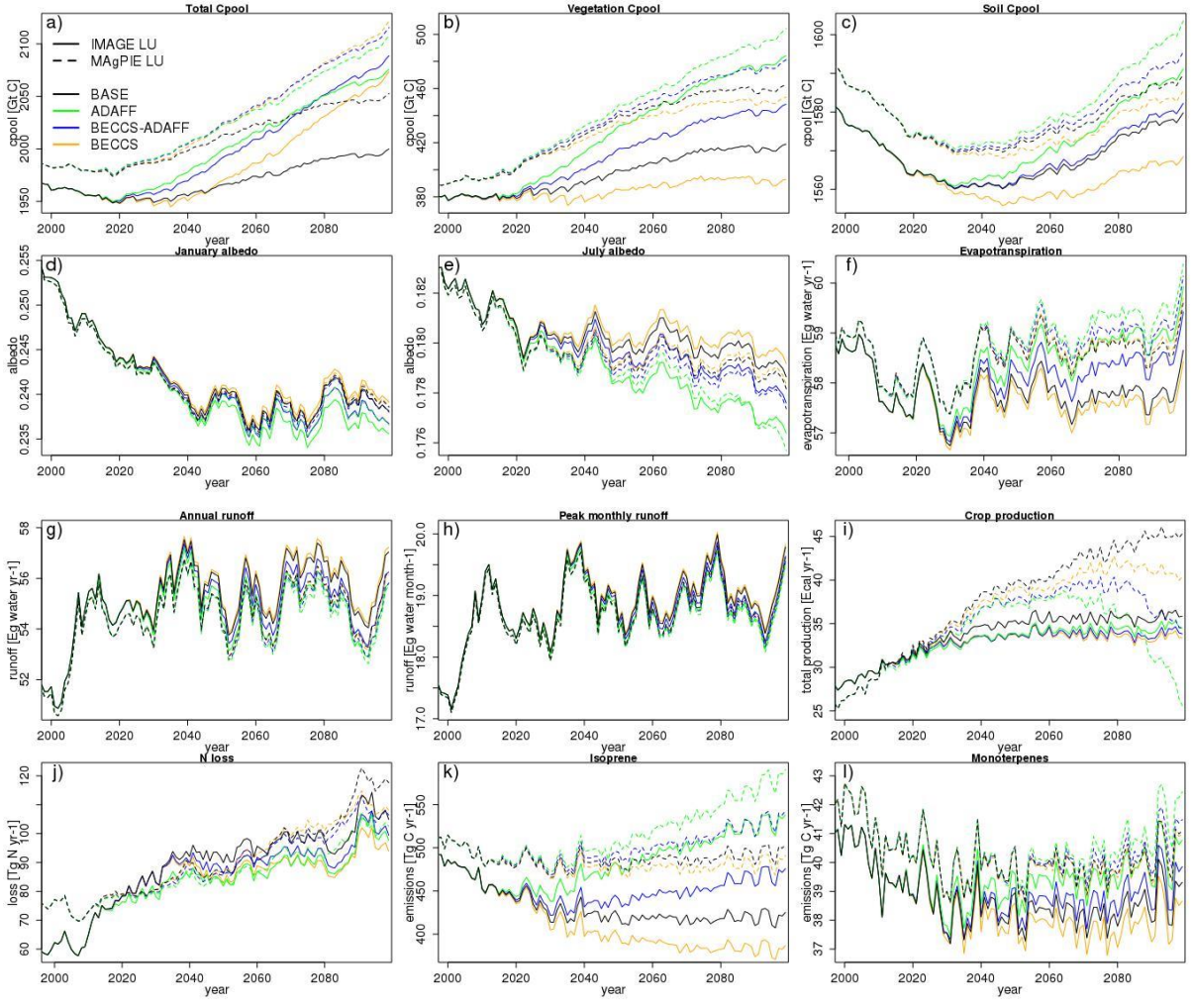

Figure A1: Time-series (2000-2099) of simulated ecosystem functions for all simulations, area-weighted and summed/averaged over all grid-cells. a) total C pool (terrestrial C, including CCS for bioenergy scenarios), b) vegetation C pool, c) soil and litter C pool, d) January albedo (5-year running mean), e) July albedo (5-year running mean), f) evapotranspiration (5-year running mean), g) annual runoff (5-year running mean), h) peak monthly runoff (5-year running mean), i) crop production, j) N loss (5-year running mean), k) isoprene emissions, l) monoterpene emissions.

Biogeosciences Discuss., doi:10.5194/bg-2017-160, 2017
Manuscript under review for journal Biogeosciences
Discussion started: 19 May 2017

Biogeosciences Discussions
Open Access
EGU

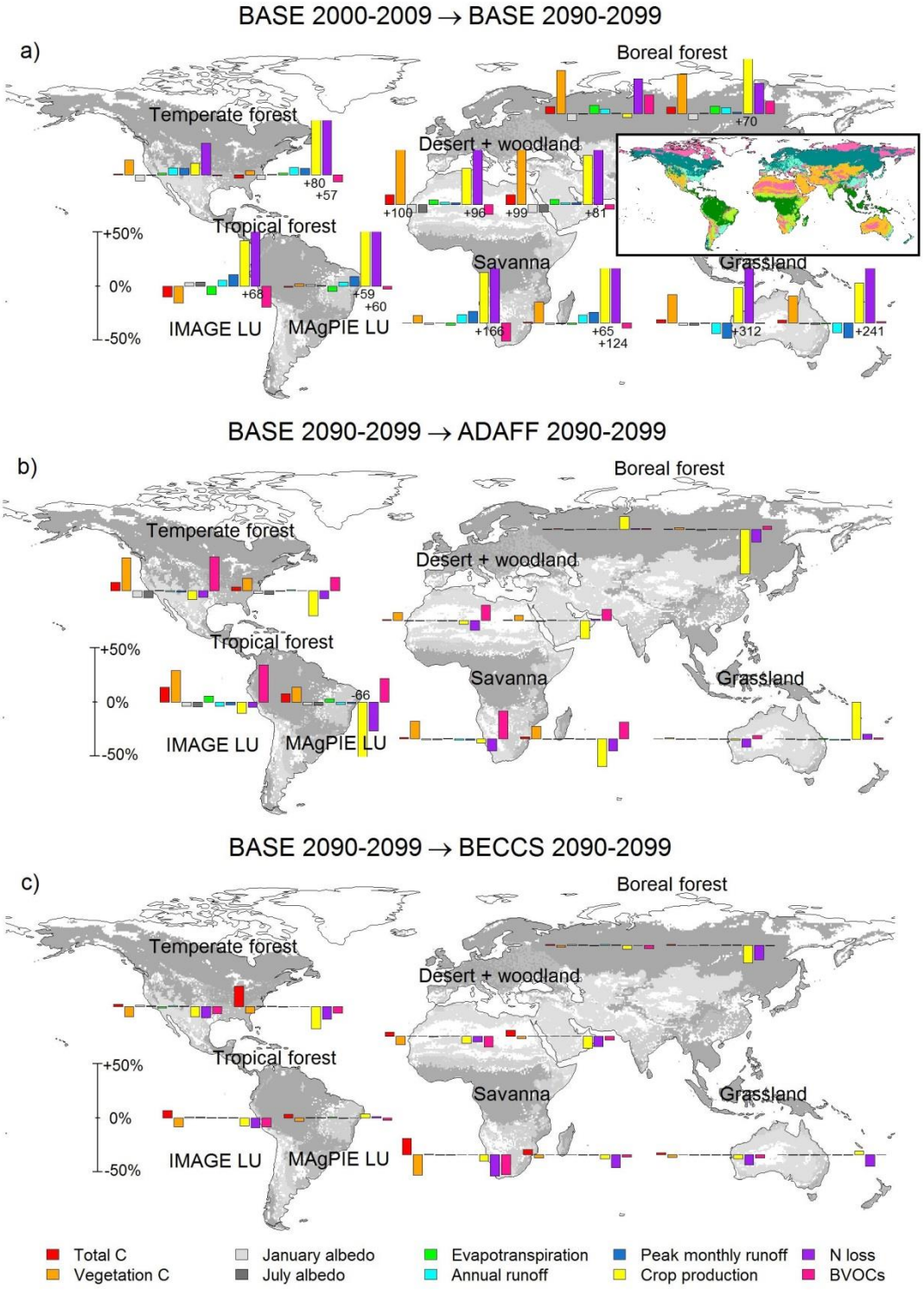

Biogeosciences Discuss., doi:10.5194/bg-2017-160, 2017
Manuscript under review for journal Biogeosciences
Discussion started: 19 May 2017

Figure A2: Same as Fig. 4 but changes shown for different biomes rather than GFED regions. Biomes are aggregated from the biomes used in Smith et al. (2014): tundra+desert+woodland+shrubland; dry+moist savanna; dry and tall grassland; tropical forest; temperate forest; boreal+temperate/boreal mixed forest. The LAI map used for the biome classification was taken from the MAgPIE BASE simulation and the 2000-2009 period. The coloured snapshot in a) shows the same biomes as the grey-coloured biomes in the larger maps to facilitate differantiation.

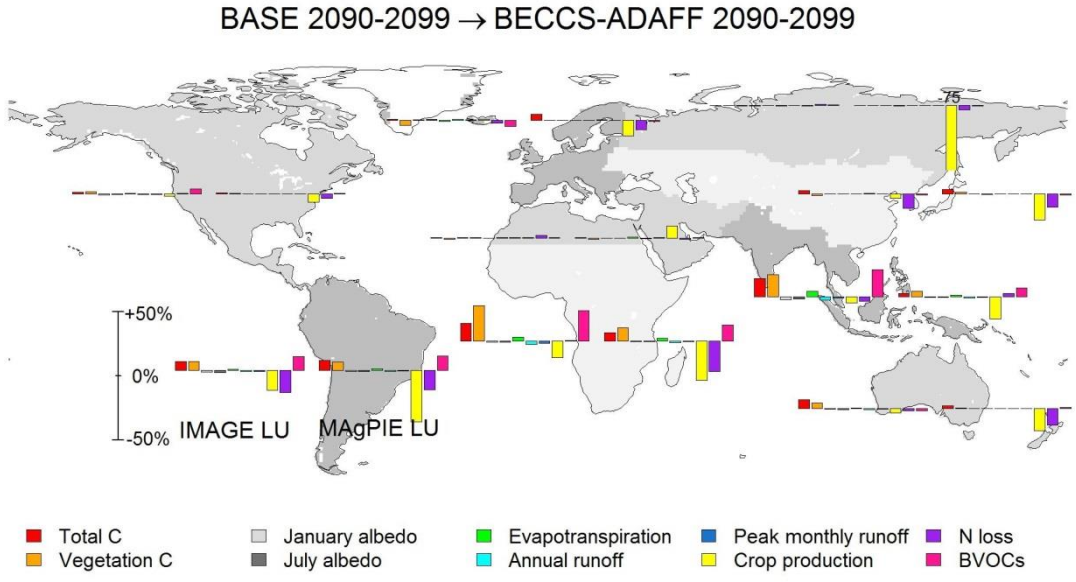

Figure A3: Regional relative changes in analyzed ecosystem functions for IMAGE LU (left) and MAgPIE LU (right) from BASE to BECCS-ADAFF by the 2090-2099 period. Changes are capped at ±50% for clarity reasons, values exceeding ±50% are written upon/below the bar. Regions are aggregated Global Fire Emissions Database regions (Giglio et al., 2010).

Biogeosciences Discuss., doi:10.5194/bg-2017-160, 2017
Manuscript under review for journal Biogeosciences
Discussion started: 19 May 2017

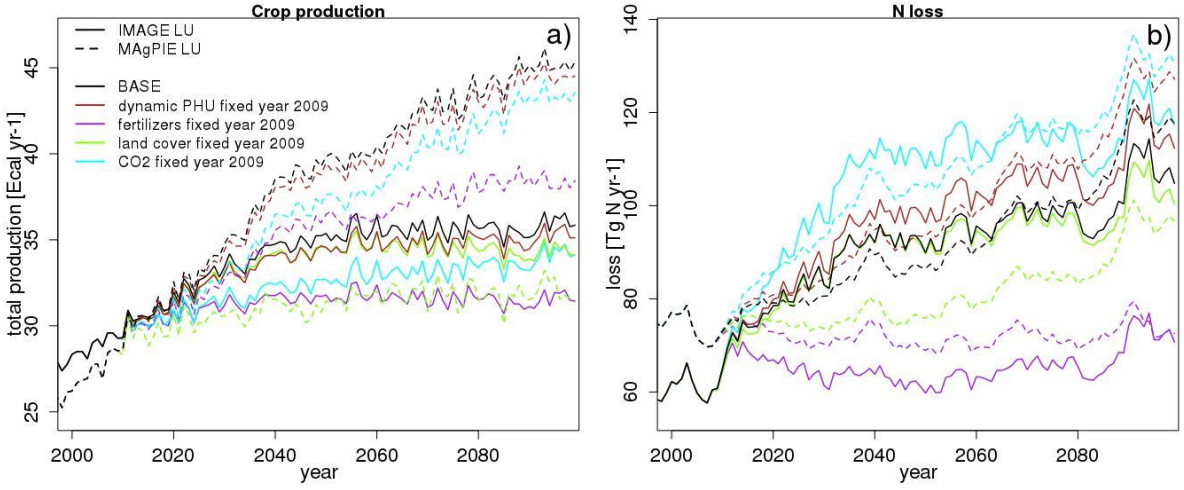

Figure A4: Impacts of fixing N fertilizers, crop area, dynamic PHU calculation (i.e. adaption to climate change via selecting suitable varieties) and atmospheric CO_2 concentration at year 2009 levels on crop production (a) and N loss (b), for the BASE simulations.

Competing interests

The authors declare that they have no conflict of interest.

Acknowledgements

This work was funded by the Helmholtz Association through the International Research Group CLUCIE and by the European Commission's 7th Framework Programme, under Grant Agreement number 603542 (LUC4C). AK, AB and AA acknowledge also support by the European Commission's 7th Framework Programme, under Grant Agreement number 308393 (OPERAs). This work was supported, in part, by the German Federal Ministry of Education and Research (BMBF), through the Helmholtz Association and its research program ATMO. It also represents paper number 22 of the Birmingham Institute of Forest Research.

References

Alkama, R., and Cescatti, A.: Biophysical climate impacts of recent changes in global forest cover, Science, 351, 600-604, doi:10.1126/science.aac8083, 2016.

Alkemade, R., van Oorschot, M., Miles, L., Nellemann, C., Bakkenes, M., and ten Brink, B.: GLOBIO3: A framework to investigate options for reducing global terrestrial biodiversity loss, Ecosystems, 12, 374–390, doi:10.1007/s10021-009-9229-5, 2009.

Anderson, K., and Peters, G.: The trouble with negative emissions, Science, 354, 182-183, doi:10.1126/science.aah4567, 2016.

Arneth, A., Harrison, S. P., Zaehle, S., Tsigaridis, K., Menon, S., Bartlein, P. J., Feichter, J., Korhola, A., Kulmala, M., O'Donnell, D., Schurgers, G., Sorvari, S., and Vesala, T.: Terrestrial biogeochemical feedbacks in the climate system, Nat Geosci, 3, 525-532, doi:10.1038/ngeo905, 2010.

Ashworth, K., Folberth, G., Hewitt, C. N., and Wild, O.: Impacts of near-future cultivation of biofuel feedstocks on atmospheric composition and local air quality, Atmos Chem Phys, 12, 919-939, doi:10.5194/acp-12-919-2012, 2012.

Bala, G., Caldeira, K., Wickett, M., Phillips, T. J., Lobell, D. B., Delire, C., and Mirin, A.: Combined climate and carbon-cycle effects of large-scale deforestation, P Natl Acad Sci USA, 104, 6550-6555, doi:10.1073/pnas.0608998104, 2007.

Ban-Weiss, G. A., Bala, G., Cao, L., Pongratz, J., and Caldeira, K.: Climate forcing and response to idealized changes in surface latent and sensible heat, Environ Res Lett, 6, doi:10.1088/1748-9326/6/3/034032, 2011.

Bathiany, S., Claussen, M., Brovkin, V., Raddatz, T., and Gayler, V.: Combined biogeophysical and biogeochemical effects of large-scale forest cover changes in the MPI earth system model, Biogeosciences, 7, 1383-1399, doi:10.5194/bg-7-1383-2010, 2010.

Behera, S. N., Sharma, M., Aneja, V. P., and Balasubramanian, R.: Ammonia in the atmosphere: a review on emission sources, atmospheric chemistry and deposition on terrestrial bodies, Environ Sci Pollut R, 20, 8092-8131, doi:10.1007/s11356-013-2051-9, 2013.

Behrman, K. D., Juenger, T. E., Kiniry, J. R., and Keitt, T. H.: Spatial land use trade-offs for maintenance of biodiversity, biofuel, and agriculture, Landscape Ecol, 30, 1987-1999, doi:10.1007/s10980-015-0225-1, 2015.

Bennett, E. M., Peterson, G. D., and Gordon, L. J.: Understanding relationships among multiple ecosystem services, Ecol Lett, 12, 1394-1404, doi:10.1111/j.1461-0248.2009.01387.x, 2009.

Betts, R. A.: Offset of the potential carbon sink from boreal forestation by decreases in surface albedo, Nature, 408, 187-190, doi:10.1038/35041545, 2000.

Blanke, J. H., Olin, S., Stürck, J., Sahlin, U., Lindeskog, M., Helming, J., and Lehsten, V.: Assessing the impact of changes in land-use intensity and climate on simulated trade-offs between crop yield and nitrogen leaching, Agriculture, Ecosystems and Environment, 239, 385-398, doi:10.1016/j.agee.2017.01.038, 2017.

Boisier, J. P., de Noblet-Ducoudre, N., and Ciais, P.: Inferring past land use-induced changes in surface albedo from satellite observations: a useful tool to evaluate model simulations, Biogeosciences, 10, 1501-1516, doi:10.5194/bg-10-1501-2013, 2013.

Bondeau, A., Smith, P. C., Zaehle, S., Schaphoff, S., Lucht, W., Cramer, W., Gerten, D., Lotze-Campen, H., Muller, C., Reichstein, M., and Smith, B.: Modelling the role of agriculture for the 20th century global terrestrial carbon balance, Global Change Biol, 13, 679-706, doi:10.1111/j.1365-2486.2006.01305.x, 2007.

Boucher, O., Myhre, G., and Myhre, A.: Direct human influence of irrigation on atmospheric water vapour and climate, Clim Dynam, 22, 597-603, doi:10.1007/s00382-004-0402-4, 2004.

Bradshaw, C. J. A., Sodhi, N. S., Peh, K. S. H., and Brook, B. W.: Global evidence that deforestation amplifies flood risk and severity in the developing world, Global Change Biol, 13, 2379-2395, doi:10.1111/j.1365-2486.2007.01446.x, 2007.

Camargo, J. A., and Alonso, A.: Ecological and toxicological effects of inorganic nitrogen pollution in aquatic ecosystems: A global assessment, Environ Int, 32, 831-849, doi:10.1016/j.envint.2006.05.002, 2006.

Carslaw, K. S., Boucher, O., Spracklen, D. V., Mann, G. W., Rae, J. G. L., Woodward, S., and Kulmala, M.: A review of natural aerosol interactions and feedbacks within the Earth system, Atmos Chem Phys, 10, 1701-1737, doi:10.5194/acp-10-1701-2010, 2010.

Creutzig, F., Ravindranath, N. H., Berndes, G., Bolwig, S., Bright, R., Cherubini, F., Chum, H., Corbera, E., Delucchi, M., Faaij, A., Fargione, J., Haberl, H., Heath, G., Lucon, O., Plevin, R., Popp, A., Robledo-Abad, C., Rose, S., Smith, P., Stromman, A., Suh, S., and Masera, O.: Bioenergy and climate change mitigation: an assessment, Gcb Bioenergy, 7, 916-944, doi:10.1111/gcbb.12205, 2015.

Creutzig, F.: Economic and ecological views on climate change mitigation with bioenergy and negative emissions, Gcb Bioenergy, 8, 4-10, doi:10.1111/gcbb.12235, 2016.

Crutzen, P. J., Mosier, A. R., Smith, K. A., and Winiwarter, W.: N2O release from agro-biofuel production negates global warming reduction by replacing fossil fuels, Atmos Chem Phys, 8, 389-395, doi:10.5194/acp-8-389-2008, 2008.

Cunningham, S. C., Mac Nally, R., Baker, P. J., Cavagnaro, T. R., Beringer, J., Thomson, J. R., and Thompson, R. M.: Balancing the environmental benefits of reforestation in agricultural regions, Perspect Plant Ecol, 17, 301-317, doi:10.1016/j.ppees.2015.06.001, 2015.

Davidson, E. A., and Kanter, D.: Inventories and scenarios of nitrous oxide emissions, Environ Res Lett, 9, doi:10.1088/1748-9326/9/10/105012, 2014.

Davies-Barnard, T., Valdes, P. J., Singarayer, J. S., Pacifico, F. M., and Jones, C. D.: Full effects of land use change in the representative concentration pathways, Environ Res Lett, 9, doi:10.1088/1748-9326/9/11/114014, 2014.

de Noblet-Ducoudre, N., Boisier, J. P., Pitman, A., Bonan, G. B., Brovkin, V., Cruz, F., Delire, C., Gayler, V., van den Hurk, B. J. J. M., Lawrence, P. J., van der Molen, M. K., Muller, C., Reick, C. H., Strengers, B. J., and Voldoire, A.: Determining Robust Impacts of Land-Use-Induced Land Cover Changes on Surface Climate over North America and Eurasia: Results from the First Set of LUCID Experiments, J Climate, 25, 3261-3281, doi:10.1175/Jcli-D-11-00338.1, 2012.

DeFries, R. S., Foley, J. A., and Asner, G. P.: Land-use choices: balancing human needs and ecosystem function, Front Ecol Environ, 2, 249-257, doi:10.1890/1540-9295(2004)002[0249:Lcbhna]2.0.Co;2, 2004.

Dellink, R., Chateau, J., Lanzi, E., and Magne, B.: Long-term economic growth projections in the Shared Socioeconomic Pathways, Global Environ Chang, 42, 200-214, doi:10.1016/j.gloenvcha.2015.06.004, 2017.

Elliott, J., Deryng, D., Mueller, C., Frieler, K., Konzmann, M., Gerten, D., Glotter, M., Florke, M., Wada, Y., Best, N., Eisner, S., Fekete, B. M., Folberth, C., Foster, I., Gosling, S. N., Haddeland, I., Khabarov, N., Ludwig, F., Masaki, Y., Olin, S., Rosenzweig, C., Ruane, A. C., Satoh, Y., Schmid, E., Stacke, T., Tang, Q. H., and Wisser, D.: Constraints and potentials of future irrigation water availability on agricultural production under climate change, P Natl Acad Sci USA, 111, 3239-3244, doi:10.1073/pnas.1222474110, 2014.

Ellison, D., Futter, M. N., and Bishop, K.: On the forest cover-water yield debate: from demand- to supply-side thinking, Global Change Biol, 18, 806-820, doi:10.1111/j.1365-2486.2011.02589.x, 2012.

Erisman, J. W., Galloway, J., Seitzinger, S., Bleeker, A., and Butterbach-Bahl, K.: Reactive nitrogen in the environment and its effect on climate change, Curr Opin Env Sust, 3, 281-290, doi:10.1016/j.cosust.2011.08.012, 2011.

Farley, K. A., Jobbagy, E. G., and Jackson, R. B.: Effects of afforestation on water yield: a global synthesis with implications for policy, Global Change Biol, 11, 1565-1576, doi:10.1111/j.1365-2486.2005.01011.x, 2005.

Ferreira, S., and Ghimire, R.: Forest cover, socioeconomics, and reported flood frequency in developing countries, Water Resour Res, 48, doi:10.1029/2011wr011701, 2012.

Fleischer, K., Warlind, D., van der Molen, M. K., Rebel, K. T., Arneth, A., Erisman, J. W., Wassen, M. J., Smith, B., Gough, C. M., Margolis, H. A., Cescatti, A., Montagnani, L., Arain, A., and Dolman, A. J.: Low historical nitrogen deposition effect on carbon sequestration in the boreal zone, J Geophys Res-Biogeo, 120, 2542-2561, doi:10.1002/2015JG002988, 2015.

Foley, J. A., DeFries, R., Asner, G. P., Barford, C., Bonan, G., Carpenter, S. R., Chapin, F. S., Coe, M. T., Daily, G. C., Gibbs, H. K., Helkowski, J. H., Holloway, T., Howard, E. A., Kucharik, C. J., Monfreda, C., Patz, J. A., Prentice, I. C., Ramankutty, N., and Snyder, P. K.: Global consequences of land use, Science, 309, 570-574, doi:10.1126/science.1111772, 2005.

Friedlingstein, P., Meinshausen, M., Arora, V. K., Jones, C. D., Anav, A., Liddicoat, S. K., and Knutti, R.: Uncertainties in CMIP5 Climate Projections due to Carbon Cycle Feedbacks, J Climate, 27, 511-526, doi:10.1175/Jcli-D-12-00579.1, 2014.

Fuchs, H., Hofzumahaus, A., Rohrer, F., Bohn, B., Brauers, T., Dorn, H. P., Haseler, R., Holland, F., Kaminski, M., Li, X., Lu, K., Nehr, S., Tillmann, R., Wegener, R., and Wahner, A.: Experimental evidence for efficient hydroxyl radical regeneration in isoprene oxidation, Nat Geosci, 6, 1023-1026, doi:10.1038/NGEO1964, 2013.

Fuss, S., Canadell, J. G., Peters, G. P., Tavoni, M., Andrew, R. M., Ciais, P., Jackson, R. B., Jones, C. D., Kraxner, F., Nakicenovic, N., Le Quere, C., Raupach, M. R., Sharifi, A., Smith, P., and Yamagata, Y.: COMMENTARY: Betting on negative emissions, Nat Clim Change, 4, 850-853, doi:10.1038/nclimate2392, 2014.

Galloway, J. N., Dentener, F. J., Capone, D. G., Boyer, E. W., Howarth, R. W., Seitzinger, S. P., Asner, G. P., Cleveland, C. C., Green, P. A., Holland, E. A., Karl, D. M., Michaels, A. F., Porter, J. H., Townsend, A. R., and Vorosmarty, C. J.: Nitrogen cycles: past, present, and future, Biogeochemistry, 70, 153-226, doi:10.1007/s10533-004-0370-0, 2004.

Ganzeveld, L., Bouwman, L., Stehfest, E., van Vuuren, D. P., Eickhout, B., and Lelieveld, J.: Impact of future land use and land cover changes on atmospheric chemistry-climate interactions, J Geophys Res-Atmos, 115, doi:10.1029/2010jd014041, 2010.

Gasser, T., Guivarch, C., Tachiiri, K., Jones, C. D., and Ciais, P.: Negative emissions physically needed to keep global warming below 2 degrees C, Nat Commun, 6, doi:10.1038/Ncomms8958, 2015.

Giglio, L., Randerson, J. T., van der Werf, G. R., Kasibhatla, P. S., Collatz, G. J., Morton, D. C., and DeFries, R. S.: Assessing variability and long-term trends in burned area by merging multiple satellite fire products, Biogeosciences, 7, 1171-1186, doi:10.5194/bg-7-1171-2010, 2010.

Hansen, R. F., Lewis, T. R., Graham, L., Whalley, S. K., Seakins, P. W., Heard, D. E., and Blitz, M. A.: OH production from the photolysis of isoprene-derived peroxy radicals: cross-sections, quantum yields and atmospheric implications, Phys. Chem. Chem. Phys, 19, 2332-2345, doi:10.1039/c6cp06718b, 2017.

Hantson, S., Knorr, W., Schurgers, G., Pugh, T. A. M., and Arneth, A.: Global isoprene and monoterpene emissions under changing climate, vegetation, CO2 and land use, Atmos Environ, 155, 35-45, doi:10.1016/j.atmosenv.2017.02.010, 2017.

Hempel, S., Frieler, K., Warszawski, L., Schewe, J., and Piontek, F.: A trend-preserving bias correction - the ISI-MIP approach, Earth Syst Dynam, 4, 219-236, doi:10.5194/esd-4-219-2013, 2013.

Hoogwijk, M., Faaija, A., van den Broek, R., Berndes, G., Gielen, D., and Turkenburg, W.: Exploration of the ranges of the global potential of biomass for energy, Biomass Bioenerg, 25, 119-133, doi:10.1016/S0961-9534(02)00191-5, 2003.

Houldcroft, C. J., Grey, W. M. F., Barnsley, M., Taylor, C. M., Los, S. O., and North, P. R. J.: New Vegetation Albedo Parameters and Global Fields of Soil Background Albedo Derived from MODIS for Use in a Climate Model, J Hydrometeorol, 10, 183-198, doi:10.1175/2008JHM1021.1, 2009.

Hua, F. Y., Wang, X. Y., Zheng, X. L., Fisher, B., Wang, L., Zhu, J. G., Tang, Y., Yu, D. W., and Wilcove, D. S.: Opportunities for biodiversity gains under the world's largest reforestation programme, Nat Commun, 7, doi:10.1038/Ncomms12717, 2016.

Humpenöder, F., Popp, A., Dietrich, J. P., Klein, D., Lotze-Campen, H., Bonsch, M., Bodirsky, B. L., Weindl, I., Stevanovic, M., and Muller, C.: Investigating afforestation and bioenergy CCS as climate change mitigation strategies, Environ Res Lett, 9, doi:10.1088/1748-9326/9/6/064029, 2014.

Jackson, R. B., Jobbagy, E. G., Avissar, R., Roy, S. B., Barrett, D. J., Cook, C. W., Farley, K. A., le Maitre, D. C., McCarl, B. A., and Murray, B. C.: Trading water for carbon with biological sequestration, Science, 310, 1944-1947, doi:10.1126/science.1119282, 2005.

Jantz, S. M., Barker, B., Brooks, T. M., Chini, L. P., Huang, Q. Y., Moore, R. M., Noel, J., and Hurtt, G. C.: Future habitat loss and extinctions driven by land-use change in biodiversity hotspots under four scenarios of climate-change mitigation, Conserv Biol, 29, 1122-1131, doi:10.1111/cobi.12549, 2015.

Kato, E., and Yamagata, Y.: BECCS capability of dedicated bioenergy crops under a future land-use scenario targeting net negative carbon emissions, Earths Future, 2, 421-439, doi:10.1002/2014EF000249, 2014.

Keller, D. P., Feng, E. Y., and Oschlies, A.: Potential climate engineering effectiveness and side effects during a high carbon dioxide-emission scenario, Nat Commun, 5, doi:10.1038/ncomms4304, 2014.

Kemper, J.: Biomass and carbon dioxide capture and storage: A review, Int J Greenh Gas Con, 40, 401-430, doi:10.1016/j.ijggc.2015.06.012, 2015.

Klein, D., Luderer, G., Kriegler, E., Strefler, J., Bauer, N., Leimbach, M., Popp, A., Dietrich, J. P., Humpenoder, F., Lotze-Campen, H., and Edenhofer, O.: The value of bioenergy in low stabilization scenarios: an assessment using REMIND-MAgPIE, Climatic Change, 123, 705-718, doi:10.1007/s10584-013-0940-z, 2014.

Klein Goldewijk, K., Beusen, A., van Drecht, G., and de Vos, M.: The HYDE 3.1 spatially explicit database of human-induced global land-use change over the past 12,000 years, Global Ecol Biogeogr, 20, 73-86, doi:10.1111/j.1466-8238.2010.00587.x, 2011.

Krause, A., Pugh, T. A. M., Bayer, A. D., Lindeskog, M., and Arneth, A.: Impacts of land-use history on the recovery of ecosystems after agricultural abandonment, Earth Syst Dynam, 7, 745-766, doi:10.5194/esd-7-745-2016, 2016.

Lamarque, J. F., Bond, T. C., Eyring, V., Granier, C., Heil, A., Klimont, Z., Lee, D., Liousse, C., Mieville, A., Owen, B., Schultz, M. G., Shindell, D., Smith, S. J., Stehfest, E., Van Aardenne, J., Cooper, O. R., Kainuma, M., Mahowald, N., McConnell, J. R., Naik, V., Riahi, K., and van Vuuren, D. P.: Historical (1850-2000) gridded anthropogenic and biomass burning emissions of reactive gases and aerosols: methodology and application, Atmos Chem Phys, 10, 7017-7039, doi:10.5194/acp-10-7017-2010, 2010.

Lamarque, J. F., Kyle, G. P., Meinshausen, M., Riahi, K., Smith, S. J., van Vuuren, D. P., Conley, A. J., and Vitt, F.: Global and regional evolution of short-lived radiatively-active gases and aerosols in the Representative Concentration Pathways, Climatic Change, 109, 191-212, doi:10.1007/s10584-011-0155-0, 2011.

Le Quere, C., Moriarty, R., Andrew, R. M., Canadell, J. G., Sitch, S., Korsbakken, J. I., Friedlingstein, P., Peters, G. P., Andres, R. J., Boden, T. A., Houghton, R. A., House, J. I., Keeling, R. F., Tans, P., Arneth, A., Bakker, D. C. E., Barbero, L., Bopp, L., Chang, J., Chevallier, F., Chini, L. P., Ciais, P., Fader, M., Feely, R. A., Gkritzalis, T., Harris, I., Hauck, J., Ilyina, T., Jain, A. K., Kato, E., Kitidis, V., Klein Goldewijk, K., Koven, C., Landschutzer, P., Lauvset, S. K., Lefevre, N., Lenton, A., Lima, I. D., Metzl, N., Millero, F., Munro, D. R., Murata, A., Nabel, J. E. M. S., Nakaoka, S., Nojiri, Y., O'Brien, K., Olsen, A., Ono, T., Perez, F. F., Pfeil, B., Pierrot, D., Poulter, B., Rehder, G., Rodenbeck, C., Saito, S., Schuster, U., Schwinger, J., Seferian, R., Steinhoff, T., Stocker, B. D., Sutton, A. J., Takahashi, T., Tilbrook, B., van der Laan-Luijkx, I. T., van der Werf, G. R., van Heuven, S., Vandemark, D., Viovy, N., Wiltshire, A., Zaehle, S., and Zeng, N.: Global Carbon Budget 2015, Earth Syst Sci Data, 7, 349-396, doi:10.5194/essd-7-349-2015, 2015.

Lelieveld, J., Butler, T. M., Crowley, J. N., Dillon, T. J., Fischer, H., Ganzeveld, L., Harder, H., Lawrence, M. G., Martinez, M., Taraborrelli, D., and Williams, J.: Atmospheric oxidation capacity sustained by a tropical forest, Nature, 452, 737-740, doi:10.1038/nature06870, 2008.

Li, Y., Zhao, M. S., Motesharrei, S., Mu, Q. Z., Kalnay, E., and Li, S. C.: Local cooling and warming effects of forests based on satellite observations, Nat Commun, 6, doi:10.1038/Ncomms7603, 2015.

Liang, J. J., Crowther, T. W., Picard, N., Wiser, S., Zhou, M., Alberti, G., Schulze, E. D., McGuire, A. D., Bozzato, F., Pretzsch, H., de-Miguel, S., Paquette, A., Herault, B., Scherer-Lorenzen, M., Barrett, C. B., Glick, H. B., Hengeveld, G. M., Nabuurs, G. J., Pfautsch, S., Viana, H., Vibrans, A. C., Ammer, C., Schall, P., Verbyla, D., Tchebakova, N., Fischer, M., Watson, J. V., Chen, H. Y. H., Lei, X. D., Schelhaas, M. J., Lu, H. C., Gianelle, D., Parfenova, E. I., Salas, C., Lee, E., Lee, B., Kim, H. S., Bruelheide, H., Coomes, D. A., Piotto, D., Sunderland, T., Schmid, B., Gourlet-Fleury, S., Sonke, B., Tavani, R., Zhu, J., Brandl, S., Vayreda, J., Kitahara, F., Searle, E. B., Neldner, V. J., Ngugi, M. R., Baraloto, C., Frizzera, L., Balazy, R., Oleksyn, J., Zawila-Niedzwiecki, T., Bouriaud, O., Bussotti, F., Finer, L., Jaroszewicz, B., Jucker, T., Valladares, F., Jagodzinski, A. M., Peri, P. L., Gonmadje, C., Marthy, W., O'Brien, T., Martin, E. H., Marshall, A. R., Rovero, F., Bitariho, R., Niklaus, P. A., Alvarez-Loayza, P., Chamuya, N., Valencia, R., Mortier, F., Wortel, V., Engone-Obiang, N. L., Ferreira, L. V., Odeke, D. E., Vasquez, R. M., Lewis, S. L., and Reich, P. B.: Positive biodiversity-productivity relationship predominant in global forests, Science, 354, 196, doi:10.1126/science.aaf8957, 2016.

Lindeskog, M., Arneth, A., Bondeau, A., Waha, K., Seaquist, J., Olin, S., and Smith, B.: Implications of accounting for land use in simulations of ecosystem carbon cycling in Africa, Earth Syst Dynam, 4, 385-407, doi:10.5194/esd-4-385-2013, 2013.

Liu, G. D., Li, Y. C., and Alva, A. K.: Moisture quotients for ammonia volatilization from four soils in potato production regions, Water Air Soil Poll, 183, 115-127, doi:10.1007/s11270-007-9361-9, 2007.

Lotze-Campen, H., Muller, C., Bondeau, A., Rost, S., Popp, A., and Lucht, W.: Global food demand, productivity growth, and the scarcity of land and water resources: a spatially explicit mathematical programming approach, Agr Econ-Blackwell, 39, 325-338, doi:10.1111/j.1574-0862.2008.00336.x, 2008.

Mace, G. M., Norris, K., and Fitter, A. H.: Biodiversity and ecosystem services: a multilayered relationship, Trends Ecol Evol, 27, 19-26, doi:10.1016/j.tree.2011.08.006, 2012.

Martin, M. V., Heald, C. L., Lamarque, J. F., Tilmes, S., Emmons, L. K., and Schichtel, B. A.: How emissions, climate, and land use change will impact mid-century air quality over the United States: a focus on effects at national parks, Atmos Chem Phys, 15, 2805-2823, doi:10.5194/acp-15-2805-2015, 2015.

Meinshausen, M., Smith, S. J., Calvin, K., Daniel, J. S., Kainuma, M. L. T., Lamarque, J. F., Matsumoto, K., Montzka, S. A., Raper, S. C. B., Riahi, K., Thomson, A., Velders, G. J. M., and van Vuuren, D. P. P.: The RCP greenhouse gas concentrations and their extensions from 1765 to 2300, Climatic Change, 109, 213-241, doi:10.1007/s10584-011-0156-z, 2011.

Millennium Ecosystem Assessment: Ecosystems and Human Well-being: Synthesis, Washington, DC, 155, 2005.

Monfreda, C., Ramankutty, N., and Foley, J. A.: Farming the planet: 2. Geographic distribution of crop areas, yields, physiological types, and net primary production in the year 2000, Global Biogeochem Cy, 22, doi:10.1029/2007gb002947, 2008.

Mueller, N. D., Gerber, J. S., Johnston, M., Ray, D. K., Ramankutty, N., and Foley, J. A.: Closing yield gaps through nutrient and water management, Nature, 490, 254-257, doi:10.1038/nature11420, 2012.

Murphy, G. E. P., and Romanuk, T. N.: A meta-analysis of declines in local species richness from human disturbances, Ecol Evol, 4, 91-103, doi:10.1002/ece3.909, 2014.

Newbold, T., Hudson, L. N., Phillips, H. R. P., Hill, S. L. L., Contu, S., Lysenko, I., Blandon, A., Butchart, S. H. M., Booth, H. L., Day, J., De Palma, A., Harrison, M. L. K., Kirkpatrick, L., Pynegar, E., Robinson, A., Simpson, J., Mace, G. M., Scharlemann, J. P. W., and Purvis, A.: A global model of the response of tropical and sub-tropical forest biodiversity to anthropogenic pressures, P Roy Soc B-Biol Sci, 281, doi:10.1098/Rspb.2014.1371, 2014.

O'Neill, B. C., Kriegler, E., Riahi, K., Ebi, K. L., Hallegatte, S., Carter, T. R., Mathur, R., and van Vuuren, D. P.: A new scenario framework for climate change research: the concept of shared socioeconomic pathways, Climatic Change, 122, 387-400, doi:10.1007/s10584-013-0905-2, 2014.

Oki, T., and Kanae, S.: Global hydrological cycles and world water resources, Science, 313, 1068-1072, doi:10.1126/science.1128845, 2006.

Olin, S., Lindeskog, M., Pugh, T. A. M., Schurgers, G., Warlind, D., Mishurov, M., Zaehle, S., Stocker, B. D., Smith, B., and Arneth, A.: Soil carbon management in large-scale Earth system modelling: implications for crop yields and nitrogen leaching, Earth Syst Dynam, 6, 745-768, doi:10.5194/esd-6-745-2015, 2015a.

Olin, S., Schurgers, G., Lindeskog, M., Warlind, D., Smith, B., Bodin, P., Holmer, J., and Arneth, A.: Modelling the response of yields and tissue C : N to changes in atmospheric CO2 and N management in the main wheat regions of western Europe, Biogeosciences, 12, 2489-2515, doi:10.5194/bg-12-2489-2015, 2015b.

Peters, G. P., Andrew, R. M., Boden, T., Canadell, J. G., Ciais, P., Le Quere, C., Marland, G., Raupach, M. R., and Wilson, C.: COMMENTARY: The challenge to keep global warming below 2 degrees C, Nat Clim Change, 3, 4-6, doi:10.1038/nclimate1783, 2013.

Peters, G. P., Andrew, R. M., Canadell, J. G., Fuss, S., Jackson, R. B., Korsbakken, J. I., Le Quere, C., and Nakicenovic, N.: Key indicators to track current progress and future ambition of the Paris Agreement, Nat Clim Change, 7, 118-123, doi:10.1038/Nclimate3202, 2017.

Popp, A., Humpenoder, F., Weindl, I., Bodirsky, B. L., Bonsch, M., Lotze-Campen, H., Muller, C., Biewald, A., Rolinski, S., Stevanovic, M., and Dietrich, J. P.: Land-use protection for climate change mitigation, Nat Clim Change, 4, 1095-1098, doi:10.1038/Nclimate2444, 2014.

Popp, A., Calvin, K., Fujimori, S., Havlik, P., Humpenoder, F., Stehfest, E., Bodirsky, B. L., Dietrich, J. P., Doelmann, J. C., Gusti, M., Hasegawa, T., Kyle, P., Obersteiner, M., Tabeau, A., Takahashi, K., Valin, H., Waldhoff, S., Weindl, I., Wise, M.,

Kriegler, E., Lotze-Campen, H., Fricko, O., Riahi, K., and van Vuuren, D. P.: Land-use futures in the shared socio-economic pathways, Global Environ Chang, 42, 331-345, doi:10.1016/j.gloenvcha.2016.10.002, 2017.

Posthumus, H., Morris, J., Hess, T. M., Neville, D., Phillips, E., and Baylis, A.: Impacts of the summer 2007 floods on agriculture in England, J Flood Risk Manag, 2, 182-189, doi:10.1111/j.1753-318X.2009.01031.x, 2009.

Pugh, T. A. M., MacKenzie, A. R., Hewitt, C. N., Langford, B., Edwards, P. M., Furneaux, K. L., Heard, D. E., Hopkins, J. R., Jones, C. E., Karunaharan, A., Lee, J., Mills, G., Misztal, P., Moller, S., Monks, P. S., and Whalley, L. K.: Simulating atmospheric composition over a South-East Asian tropical rainforest: performance of a chemistry box model, Atmos Chem Phys, 10, 279-298, doi:10.5194/acp-10-279-2010, 2010.

Pugh, T. A. M., Arneth, A., Olin, S., Ahlström, A., Bayer, A. D., Klein Goldewijk, K., Lindeskog, M., and Schurgers, G.: Simulated carbon emissions from land use change are substantially enhanced by accounting for agricultural management, Environ Res Lett, 10, doi:10.1088/1748-9326/10/12/124008, 2015.

Pyle, J. A., Warwick, N. J., Harris, N. R. P., Abas, M. R., Archibald, A. T., Ashfold, M. J., Ashworth, K., Barkley, M. P., Carver, G. D., Chance, K., Dorsey, J. R., Fowler, D., Gonzi, S., Gostlow, B., Hewitt, C. N., Kurosu, T. P., Lee, J. D., Langford, S. B., Mills, G., Moller, S., MacKenzie, A. R., Manning, A. J., Misztal, P., Nadzir, M. S. M., Nemitz, E., Newton, H. M., O'Brien, L. M., Ong, S., Oram, D., Palmer, P. I., Peng, L. K., Phang, S. M., Pike, R., Pugh, T. A. M., Rahman, N. A., Robinson, A. D., Sentian, J., Abu Samah, A., Skiba, U., Ung, H. E., Yong, S. E., and Young, P. J.: The impact of local surface changes in Borneo on atmospheric composition at wider spatial scales: coastal processes, land-use change and air quality, Philos T R Soc B, 366, 3210-3224, doi:10.1098/rstb.2011.0060, 2011.

Reiner, D. M.: Learning through a portfolio of carbon capture and storage demonstration projects, Nat Energy, 1, doi:10.1038/Nenergy.2015.11, 2016.

Rodriguez, J. P., Beard, T. D., Bennett, E. M., Cumming, G. S., Cork, S. J., Agard, J., Dobson, A. P., and Peterson, G. D.: Trade-offs across space, time, and ecosystem services, Ecol Soc, 11, 2006.

Rogelj, J., Luderer, G., Pietzcker, R. C., Kriegler, E., Schaeffer, M., Krey, V., and Riahi, K.: Energy system transformations for limiting end-of-century warming to below 1.5 degrees C, Nat Clim Change, 5, 519–527, doi:10.1038/nclimate2572, 2015.

Rosenkranz, M., Pugh, T. A. M., Schnitzler, J. P., and Arneth, A.: Effect of land-use change and management on biogenic volatile organic compound emissions - selecting climate-smart cultivars, Plant Cell Environ, 38, 1896-1912, doi:10.1111/pce.12453, 2015.

Samir, K. C., and Lutz, W.: The human core of the shared socioeconomic pathways: Population scenarios by age, sex and level of education for all countries to 2100, Global Environ Chang, 42, 181-192, doi:10.1016/j.gloenvcha.2014.06.004, 2017.

Sampaio, G., Nobre, C., Costa, M. H., Satyamurty, P., Soares, B. S., and Cardoso, M.: Regional climate change over eastern Amazonia caused by pasture and soybean cropland expansion, Geophys Res Lett, 34, doi:10.1029/2007gl030612, 2007.

Santangeli, A., Toivonen, T., Pouzols, F. M., Pogson, M., Hastings, A., Smith, P., and Moilanen, A.: Global change synergies and trade-offs between renewable energy and biodiversity, Gcb Bioenergy, 8, 941-951, doi:10.1111/gcbb.12299, 2016.

Scott, C. E., Rap, A., Spracklen, D. V., Forster, P. M., Carslaw, K. S., Mann, G. W., Pringle, K. J., Kivekas, N., Kulmala, M., Lihavainen, H., and Tunved, P.: The direct and indirect radiative effects of biogenic secondary organic aerosol, Atmos Chem Phys, 14, 447-470, doi:10.5194/acp-14-447-2014, 2014.

Scott, V., Haszeldine, R. S., Tett, S. F. B., and Oschlies, A.: Fossil fuels in a trillion tonne world, Nat Clim Change, 5, 419-423, doi:10.1038/Nclimate2578, 2015.

Searle, S. Y., and Malins, C. J.: Will energy crop yields meet expectations?, Biomass Bioenerg, 65, 3-12, doi:10.1016/j.biombioe.2014.01.001, 2014.

Sillman, S.: The relation between ozone, NOx and hydrocarbons in urban and polluted rural environments, Atmos Environ, 33, 1821-1845, doi:10.1016/S1352-2310(98)00345-8, 1999.

Slade, R., Bauen, A., and Gross, R.: Global bioenergy resources, Nat Clim Change, 4, 99-105, doi:10.1038/Nclimate2097, 2014.

Smith, B., Warlind, D., Arneth, A., Hickler, T., Leadley, P., Siltberg, J., and Zaehle, S.: Implications of incorporating N cycling and N limitations on primary production in an individual-based dynamic vegetation model, Biogeosciences, 11, 2027-2054, doi:10.5194/bg-11-2027-2014, 2014.

Smith, L. J., and Torn, M. S.: Ecological limits to terrestrial biological carbon dioxide removal, Climatic Change, 118, 89-103, doi:10.1007/s10584-012-0682-3, 2013.

Smith, P., Ashmore, M. R., Black, H. I. J., Burgess, P. J., Evans, C. D., Quine, T. A., Thomson, A. M., Hicks, K., and Orr, H. G.: The role of ecosystems and their management in regulating climate, and soil, water and air quality, J Appl Ecol, 50, 812-829, doi:10.1111/1365-2664.12016, 2013.

Smith, P., Davis, S. J., Creutzig, F., Fuss, S., Minx, J., Gabrielle, B., Kato, E., Jackson, R. B., Cowie, A., Kriegler, E., van Vuuren, D. P., Rogelj, J., Ciais, P., Milne, J., Canadell, J. G., McCollum, D., Peters, G., Andrew, R., Krey, V., Shrestha, G., Friedlingstein, P., Gasser, T., Grubler, A., Heidug, W. K., Jonas, M., Jones, C. D., Kraxner, F., Littleton, E., Lowe, J., Moreira, J. R., Nakicenovic, N., Obersteiner, M., Patwardhan, A., Rogner, M., Rubin, E., Sharifi, A., Torvanger, A., Yamagata, Y., Edmonds, J., and Cho, Y.: Biophysical and economic limits to negative CO2 emissions, Nat Clim Change, 6, 42-50, doi:10.1038/Nclimate2870, 2016.

Stehfest, E., van Vuuren, D., Kram, T., Bouwman, L., Alkemade, R., Bakkenes, M., Biemans, H., Bouwman, A., den Elzen, M., Janse, J., Lucas, P., van Minnen, J., Müller, C., and Prins, A.: Integrated Assessment of Global Environmental Change with IMAGE 3.0 : Model description and policy applications, The Hague: PBL Netherlands Environmental Assessment Agency, 2014.

Tilman, D., Cassman, K. G., Matson, P. A., Naylor, R., and Polasky, S.: Agricultural sustainability and intensive production practices, Nature, 418, 671-677, doi:10.1038/nature01014, 2002.

Unger, N.: Human land-use-driven reduction of forest volatiles cools global climate, Nat Clim Change, 4, 907-910, doi:10.1038/nclimate2347, 2014.

Valin, H., Sands, R. D., van der Mensbrugghe, D., Nelson, G. C., Ahammad, H., Blanc, E., Bodirsky, B., Fujimori, S., Hasegawa, T., Havlik, P., Heyhoe, E., Kyle, P., Mason-D'Croz, D., Paltsev, S., Rolinski, S., Tabeau, A., van Meijl, H., von Lampe, M., and Willenbockel, D.: The future of food demand: understanding differences in global economic models, Agr Econ-Blackwell, 45, 51-67, doi:10.1111/agec.12089, 2014.

van Dijk, A. I. J. M., van Noordwijk, M., CaldeR, I. R., Bruijnzeel, S. L. A., Schellekens, J., and Chappell, N. A.: Forest-flood relation still tenuous - comment on 'Global evidence that deforestation amplifies flood risk and severity in the developing world' by Bradshaw et al., Global Change Biol, 15, 110-115, doi:10.1111/j.1365-2486.2008.01708.x, 2009.

van Vuuren, D. P., Edmonds, J., Kainuma, M., Riahi, K., Thomson, A., Hibbard, K., Hurtt, G. C., Kram, T., Krey, V., Lamarque, J. F., Masui, T., Meinshausen, M., Nakicenovic, N., Smith, S. J., and Rose, S. K.: The representative concentration pathways: an overview, Climatic Change, 109, 5-31, doi:10.1007/s10584-011-0148-z, 2011.

van Vuuren, D. P., Deetman, S., van Vliet, J., van den Berg, M., van Ruijven, B. J., and Koelbl, B.: The role of negative CO2 emissions for reaching 2 degrees C-insights from integrated assessment modelling, Climatic Change, 118, 15-27, doi:10.1007/s10584-012-0680-5, 2013.

Viglizzo, E. F., Paruelo, J. M., Laterra, P., and Jobbagy, E. G.: Ecosystem service evaluation to support land-use policy, Agr Ecosyst Environ, 154, 78-84, doi:10.1016/j.agee.2011.07.007, 2012.

Visconti, P., Pressey, R. L., Giorgini, D., Maiorano, L., Bakkenes, M., Boitani, L., Alkemade, R., Falcucci, A., Chiozza, F., and Rondinini, C.: Future hotspots of terrestrial mammal loss, Philosophical Transactions of the Royal Society B: Biological Sciences, 366, 2693–2702, doi:10.1098/rstb.2011.0105.0, 2011.

Wang, Z., and Zeng, X. B.: Evaluation of Snow Albedo in Land Models for Weather and Climate Studies, J Appl Meteorol Clim, 49, 363-380, doi:10.1175/2009JAMC2134.1, 2010.

Warszawski, L., Frieler, K., Huber, V., Piontek, F., Serdeczny, O., and Schewe, J.: The Inter-Sectoral Impact Model Intercomparison Project (ISI-MIP): Project framework, P Natl Acad Sci USA, 111, 3228-3232, doi:10.1073/pnas.1312330110, 2014.

Whitehead, P. G., Wilby, R. L., Battarbee, R. W., Kernan, M., and Wade, A. J.: A review of the potential impacts of climate change on surface water quality, Hydrolog Sci J, 54, 101-123, doi:10.1623/hysj.54.1.101, 2009.

Wilkinson, S., Mills, G., Illidge, R., and Davies, W. J.: How is ozone pollution reducing our food supply?, J Exp Bot, 63, 527-536, doi:10.1093/jxb/err317, 2012.

Williamson, P.: Scrutinize CO2 removal methods, Nature, 530, 153-155, doi:10.1038/530153a, 2016.

Wiltshire, A., and Davies-Barnard, T.: Planetary limits to BECCS negative emissions, AVOID2 WPD.2a Report 1, 2015.